

Toward Globally Optimal State Estimation Using Automatically Tightened Semidefinite Relaxations

Frederike Dümbsen Connor Holmes Ben Agro Timothy D. Barfoot

Abstract—In recent years, semidefinite relaxations of common optimization problems in robotics have attracted growing attention due to their ability to provide globally optimal solutions. In many cases, specific handcrafted redundant constraints are added to the relaxation in order to improve its tightness, which is usually a requirement for obtaining or certifying globally optimal solutions. These constraints are formulation-dependent and typically require a lengthy manual process to find. Instead, the present paper suggests an automatic method to find a set of sufficient redundant constraints to obtain tightness, if they exist. We first propose an efficient feasibility check to determine if a given set of variables can lead to a tight formulation. Secondly, we show how to scale the method to problems of bigger size. At no point of the entire process do we have to manually find redundant constraints. We showcase the effectiveness of the approach by providing new insights on two classical robotics problems: range-based localization and stereo-based pose estimation. Finally, we reproduce semidefinite relaxations presented in recent literature and show that our automatic method finds a smaller set of constraints sufficient for tightness than previously considered.

Index Terms—Optimization and optimal control, localization, certifiable algorithms, global optimality, Lagrangian duality

I. INTRODUCTION

Many problems encountered in robotic state estimation, such as calibration and simultaneous localization and mapping (SLAM), are typically posed as nonlinear least-squares optimization problems [1, 2]. Widely adopted solvers used to tackle these problems, such as Gauss-Newton (GN) and Levenberg-Marquardt (LM), have only local, if any, convergence guarantees and may terminate in suboptimal solutions [3].

Over the past years, there has been a growing effort to exploit semidefinite relaxations of these optimization problems. Semidefinite relaxations open the door to global optimality in at least two different ways: in certain cases, a (convex) semidefinite program (SDP) (or a sequence thereof) may be solved instead of the original nonconvex problem to find the globally optimal solution [4, 5, 6, 7]. In other cases, the Lagrangian dual of the SDP offers the possibility to construct so-called ‘optimality certificates’ [8, 9] to determine the global optimality of the solutions obtained by local solvers.

The performance and feasibility of the aforementioned methods greatly depends on whether the SDP relaxation is tight. For example, the globally optimal solution to the original problem can only be extracted from the SDP solution when it is rank one, in which case the relaxation is tight [8, 5, 10].

All authors are with the University of Toronto Robotics Institute, University of Toronto, Canada. Corresponding author: frederike.dumbngen@utoronto.ca

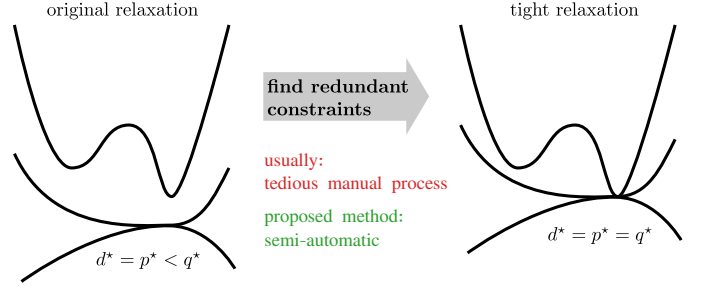


Fig. 1: The proposed method in a nutshell: we circumvent the lengthy process of finding redundant constraints to tighten a given semidefinite relaxation, using instead a sampling-based approach to automatically find all possible constraints. This allows for the quick evaluation of different formulations and substitutions of a given optimization problem, hopefully lowering the barrier for SDPs to be more widely adopted for finding globally optimal solutions to optimization problems in robotics.

Similarly, certifiable algorithms work only when strong duality obtains [11], *i.e.*, when the cost the relaxed problem solution equals the cost of the original problem [8, 5]. Tightness can also be a computational advantage; some state-of-the-art SDP solvers, for instance, work only for problems with low-rank optimal solutions [12, 6].

One important enabler for tight relaxations has been a mathematical framework called *Lasserre’s hierarchy* [13]. Put simply, the hierarchy consists of a sequence of semidefinite relaxations where polynomial substitutions of increasing order are added to the original problem. Calling the original variable dimension d and the hierarchy order k , each level results in a N_k -dimensional SDP, with $N_k := \binom{d+k}{k}$. Astonishingly, under weak technical assumptions, any problem that can be written as a polynomial optimization problem (POP) can be ‘lifted’ to a high enough order k to allow for a tight relaxation. In theory, the required order may be infinite, but many follow-up works have shown that tightness is obtained within a few hierarchy levels only [14, 8, 15, 16]. More recently, it has been shown that many problems admit a *sparse Lasserre’s hierarchy*, meaning that only some of the N_k terms may be required at each level [17, 7].

As SDPs scale poorly with problem dimension, it is desirable to achieve tightness with as few additional higher-order substitutions as possible (ideally, with none). For this matter, it has been shown that so-called redundant constraints are paramount [8, 10, 14]. However, to this date, these constraints are usually the result of a lengthy manual search process and it is often hard to retrace how the constraints were discovered [14]. In [7], a method to find all ‘trivially satisfied’

constraints is provided, but not all of these constraints may be necessary, and important constraints might be missed. To make matters worse, using different formulations may lead to entirely different forms and numbers of required redundant constraints. Due to the lack of a systematic method of finding the right formulation and sufficient redundant constraints, practitioners often have to spend great effort in trial-and-error reformulations. This adds significant overhead as opposed to easy-to-use local solvers, and thus may hinder the wide adoption of SDP methods in robotics.

In this paper, we provide tools that help automate the search for redundant constraints required for tightness. In particular, the proposed methods allow us to

- 1) determine, in only a few lines of code, if a problem in a given form can be tightened by adding enough redundant constraints. Notably, no manual steps for guessing the redundant constraints are required. This step is purposefully kept simple, allowing for quick evaluation of any problem in a given formulation (AUTOTIGHT).
- 2) automatically determine a set of ‘constraint templates’ that can be generalized to any number of variables, requiring again no need to explicitly model or interpret the found constraints (AUTOTEMPLATE).

The focus of AUTOTIGHT is feasibility and it should be performed on a small example problem. The focus of AUTOTEMPLATE is scalability, enabling to generalize the findings from AUTOTIGHT to problems of any size, which is a hard requirement for typically high-dimensional problems encountered in robotics.

The only prerequisite for using the provided tools is a method of randomly generating many problem setups (also called a ‘sampling oracle’ in the literature [18]). We believe that most roboticists generate such a method as part of their standard development process, and if not, can do so fairly easily in only a few lines of code.

This paper is structured as follows. We put the proposed method in context with related work in Section II. Then, we introduce mathematical preliminaries for relaxing a non-linear least-squares problem to an SDP in Section III. In Section IV, we present our method to determine the feasibility of tightening a given problem. Building on this method, in Section V we propose a scalable method for determining constraint templates that can be applied to any number of variables. We use the methods to provide novel insights on two state-estimation problems in Sections VI-B and VI-C, and on previously studied relaxations in VI-D. We conclude with a discussion and open research questions in Section VII.

II. RELATED WORK

The list of problems in robotics and computer vision that have been solved using semidefinite relaxations is long and continues to grow. In vision-based state estimation, semidefinite relaxations have been widely explored, for example to solve rotation averaging [19, 20, 21] or to perform camera pose estimation from pixel measurements [10, 22]. The first theoretical guarantees on tightness of these and other problems were given in [23, 9]. A set of analytical redundant

constraints that successfully tightens many problem instances involving rotations has been proposed in [24, 10] and used successfully in follow-up works to certify, for instance, hand-eye calibration [25] and generalized-essential-matrix estimation [26]. Follow-up works have shown that tight relaxations can be achieved for robust cost functions, too, which account for outliers [16, 8]. A great overview of many successfully tightened problems and robust cost functions is given in [7], in which a recipe for constructing trivially satisfied redundant constraints is also provided. Robotics planning and control problems have recently also seen a surge of relaxation-based methods [15, 27, 28]. Notably, specific redundant constraints (again, analytically specified) were found to be paramount for tightness in [28].

For some problems, no redundant constraints are required for tightness. For these problems, methods based on the *Burer Monteiro* approach [29] and the *Riemannian staircase* [30] have been shown to be extremely effective at finding the optimal solution with speeds competitive with efficient local solvers [4, 5, 31, 32]. Other methods have explored fast global optimality certificates of solutions of local solvers [33, 34]. To date, whenever redundant constraints are required for tightness, SDP solvers are generally too slow for real-time performance [7]. However, recent advances have shown that solvers can be significantly sped up when the optimal solution is of low rank [35, 6, 7]. More progress in finding faster SDP solvers for these convex relaxations is a requirement to enable the large-scale adoption of SDPs for robotics; another requirement is finding the necessary redundant constraints for a larger class of problems. We hope that the method proposed in this paper contributes to the latter.

Recently, a sampling paradigm has been explored in the sums-of-squares (SOS) literature to overcome some of the limitations of SDP solvers [18].¹ The authors suggest to sample feasible points of an SOS program and to solve an SDP including only a minimally required number of samples. The method thus implicitly exploits coordinate ring structure of the variety without the use of advanced concepts such as Grobner bases [36]. This solution has been picked up and shown great promise on small problems [37]. We use a similar paradigm in this paper, but instead of solving a sampling-based SDP, we use the samples to find generalizable constraints. Not only does this provide more insight into the kind of redundant constraints required to tighten standard SDP problems of a wide range of problems, it also allows us to generalize to novel, higher-dimensional problems.

III. PRELIMINARIES

A. Notation

We denote vectors and matrices by bold-face lowercase and uppercase letters, respectively. The transpose of matrix \mathbf{A} is written as \mathbf{A}^\top . The identity matrix in d dimensions is \mathbf{I}_d , and vector \mathbf{e}_d is the d -th standard basis vector (the d -th column of the identity matrix). A positive-semidefinite (PSD) matrix

¹There is a tight connection between the SOS relaxation and Lasserre’s hierarchy (also called moment relaxation in this context); a clear description of this connection is given in [21].

is written as $\mathbf{X} \succeq 0$, and we denote the space of $N \times N$ PSD matrices by \mathbb{S}_+^N . The inner product is denoted by $\langle \cdot, \cdot \rangle$, and the matrix inner product is defined as $\langle \mathbf{A}, \mathbf{B} \rangle = \text{tr}(\mathbf{A}^\top \mathbf{B})$ where $\text{tr}(\cdot)$ is the trace operator. We introduce $\text{vech}(\cdot)$ which extracts the elements of the upper-triangular part of a matrix, and divides the diagonal elements by $\sqrt{2}$. This ensures that $\langle \mathbf{A}, \mathbf{B} \rangle = \text{vech}(\mathbf{A})^\top \text{vech}(\mathbf{B})$, and is commonly used in SDP solvers [38]. We denote the inverse operation by $\text{vech}^{-1}(\cdot)$. $\mathbf{x}[k]$ denotes the k -th element of vector \mathbf{x} . For shorter notation, we use $[N]$ for the index set $\{1, \dots, N\}$.

B. Semi-definite Relaxations

In the remainder of this section, we provide theoretical background on semidefinite relaxations and duality theory necessary to understand this paper for the nonexpert reader. For an in-depth introduction to these topics we refer to [11, 3].

Most generally speaking, the subject of this paper is optimization problems of the form

$$\min_{\boldsymbol{\theta} \in \mathbb{R}^d} \{c(\boldsymbol{\theta}) \mid h_i(\boldsymbol{\theta}) = 0, i \in [N_h]\}, \quad (1)$$

where $\boldsymbol{\theta}$ is a decision variable, $c(\cdot)$ is the cost, and $h_i(\cdot)$ are equality constraints.² In robotics, the cost is most commonly a (robust) least-squares cost function, and the constraints may enforce the nature of the decision variables, such as $SO(3)$ for rotations or $SE(3)$ for poses [2].

The problems in which we are interested can be ‘lifted’ to a quadratically constrained quadratic program (QCQP). This includes, for instance, any POP; we show examples of a quartic and a rational cost function in Section VI. For such problems, we can rewrite (1) as

$$\min_{\mathbf{x} \in \mathbb{R}^N} \{f(\mathbf{x}) \mid g_i(\mathbf{x}) = 0, l_j(\mathbf{x}) = 0, i \in [N_h], j \in [N_l]\}, \quad (2)$$

where f and g_i are now quadratic in the lifted vector \mathbf{x} . The lifted vector is given by

$$\mathbf{x}^\top = [1 \quad \boldsymbol{\theta}^\top \quad z_1 \quad \dots \quad z_{N_l}], \quad (3)$$

where we have introduced $z_l := \ell_l(\boldsymbol{\theta})$, higher-order lifting functions of $\boldsymbol{\theta}$. By choosing enough of these substitutions, we can enforce that each substitution can itself be written as a quadratic constraint: $l_j(\mathbf{x}) = 0$. We have also added h in (3) as a homogenization variable, allowing constant and linear functions to be written as quadratic functions. We illustrate these concepts in the following example:

Example (stereo-1D). *Inspired by stereo-based localization problems, which typically involve rational cost functions, we propose the following pedagogical example problem:*

$$\min_{\boldsymbol{\theta}} \sum_{i=1}^N \left(\frac{1}{(\boldsymbol{\theta} - a_i)} \right)^2, \quad (4)$$

²We focus on equality constraints here for the sake of clarity. Note that inequality constraints can be added as long as they can also be written as quadratic constraints in the lifted vector and thus carried forward as quadratic inequality constraints in the relaxations. We include one example of inequality constraints in Section VI-D.

where $\boldsymbol{\theta} \in \mathbb{R}$ is the decision variable, and $a_i \in \mathbb{R}$ are known. Using the lifted vector

$$\mathbf{x}^\top = [h \quad \boldsymbol{\theta} \quad z_1 \quad \dots \quad z_N], \quad z_i = \ell_i(\boldsymbol{\theta}) := \frac{1}{\boldsymbol{\theta} - a_i}, \quad (5)$$

we can rewrite (24) in the form (2), with $f(\mathbf{x}) = \sum_{i=1}^N \mathbf{x}[2+i]^2$, and $l_i(\mathbf{x}) = \mathbf{x}[2+i]\mathbf{x}[1] - \mathbf{x}[2+i]a_i = 0$, which are both quadratic functions in the lifted variable $\mathbf{x}^\top = [1 \quad \boldsymbol{\theta} \quad z_1 \quad \dots \quad z_N]$.

Since all functions in (2) are quadratic in the lifted vector, we can now rewrite (2) as

$$\min_{\mathbf{x} \in \mathbb{R}^N} \{ \mathbf{x}^\top \mathbf{Q} \mathbf{x} \mid \mathbf{x}^\top \mathbf{A}_0 \mathbf{x} = 1, \mathbf{x}^\top \mathbf{A}_i \mathbf{x} = 0, i \in [N_A] \}, \quad (6)$$

where \mathbf{Q} and $\mathbf{A}_i, i \in [N_A]$ are the cost and constraint matrices, respectively, and $N_A = N_h + N_l$. The matrix \mathbf{A}_0 enforces the homogenization variable through the constraint $\mathbf{x}[1]^2 = 1$.³ We call the constraints in (6) the ‘primary constraints’.

Example (stereo-1D, cont’d). *The cost and constraints matrices for the toy stereo problem are zero except for $\mathbf{Q}[i, i] = 1$ for $i = 3 \dots N+2$ and $\mathbf{A}_i[1, 2+i] = \mathbf{A}_i[2+i, 1] = -a_i$ and $\mathbf{A}_i[2, 2+i] = \mathbf{A}_i[2+i, 2] = 1$.*

Problem (6) is a QCQP. Its solution space, defined by a set of polynomial equality constraints, defines a real algebraic variety, which is a central object of the field of algebraic geometry. This is by itself an active area of research, with methods existing for finding, for example, the minimal set of constraints to uniquely define a variety [36]. For the proposed paper, no knowledge of these advanced concepts is required as we take a numerical approach rather than an algebraic approach to describe the varieties. For the interested reader, we do include some references to the algebraic geometry perspective in footnotes.

Because (6) is, in general, NP-hard to solve, a common strategy is to relax the problem to a SDP by introducing $\mathbf{X} := \mathbf{x}\mathbf{x}^\top$, which can be enforced using $\mathbf{X} \succeq 0, \text{rank}(\mathbf{X}) = 1$, where the semidefinite constraint is convex while the rank constraint is not. We can solve the following standard SDP, also called the primal relaxation of (6):

$$\min_{\mathbf{X} \in \mathbb{S}_+^N} \{ \langle \mathbf{Q}, \mathbf{X} \rangle \mid \langle \mathbf{A}_0, \mathbf{X} \rangle = 1, \langle \mathbf{A}_i, \mathbf{X} \rangle = 0, i \in [N_A] \}, \quad (7)$$

which is the rank-relaxation of (6) (i.e., we relax the $\text{rank}(\mathbf{X}) = 1$ constraint).

C. Duality Theory and Global Optimality

The SDP problem can be used in several ways to make claims about the global optimality of candidate solutions. Let us denote by \mathbf{X}^* the solution of (7) and its associated cost by $p^* := \langle \mathbf{Q}, \mathbf{X}^* \rangle$. If \mathbf{X}^* has rank one, then it can be factored as $\mathbf{X}^* = \mathbf{x}^* \mathbf{x}^{*\top}$ and \mathbf{x}^* is the optimal solution to (6) with $q^* := f(\mathbf{x}^*) = p^*$. This leads us to the first form of tightness used in this paper.

³Technically, the first element of \mathbf{x} may thus take the value -1 , but this does not pose a problem as the whole vector can then be simply negated.

Definition 1 (Rank-tightness of the SDP relaxation). *We call the SDP relaxation (7) rank-tight if its optimal solution \mathbf{X}^* has rank one.*

SDPs also enjoy a well-understood duality theory, which makes them great candidates for so-called ‘optimality certificates’. The Lagrangian dual problem of (7) is given by

$$d^* = \max_{\rho, \lambda} \{-\rho \mid \mathbf{H}(\rho, \lambda) := \mathbf{Q} + \rho \mathbf{A}_0 + \sum_{i=1}^{N_A} \lambda_i \mathbf{A}_i \succeq 0\}, \quad (8)$$

where $\rho, \lambda \in \mathbb{R}^{N_A}$ are the Lagrangian dual variables corresponding to \mathbf{A}_0 and $\mathbf{A}_i, i \in [N_A]$, respectively. It is well known that we always have $d^* \leq p^* \leq q^*$ (see left graph of Figure 1 for a graphical depiction). In what follows, we will also make the assumption that $d^* = p^*$ which holds under common constraint qualifications such as *Slater’s condition* [11].

We can use the dual problem to, instead of solving the primal SDP and checking the rank of the solution, certify a local candidate solution $\hat{\mathbf{x}}$. Indeed, using the Karush-Kuhn-Tucker (KKT) conditions of (8), it is well-known (see e.g., [39]) that a solution candidate $\hat{\mathbf{x}}$ is globally optimal if there exist $\hat{\rho}, \hat{\lambda}$ such that

$$\begin{cases} \mathbf{H}(\hat{\rho}, \hat{\lambda}) \hat{\mathbf{x}} = \mathbf{0}, \\ \mathbf{H}(\hat{\rho}, \hat{\lambda}) \succeq 0. \end{cases} \quad (9)$$

If these two conditions hold, we have *strong duality*, meaning that $d^* = p^* = q^*$ (right plot of Figure 1). If we do not have strong duality, the above conditions cannot be jointly satisfied and we cannot make claims about the global optimality of a candidate solution. Therefore, we introduce the notion of *cost-tightness*, a weaker form of tightness than rank-tightness,⁴ which allows for candidate solutions to be certified:

Definition 2 (Cost-tightness of the SDP relaxation). *We call the SDP relaxation (7) cost-tight if $d^* = p^* = q^*$.*

Both forms of tightness may be useful in practice: when we have rank-tightness, we can solve the SDP and derive the optimal value of the QCQP from it. When the SDP is prohibitively large, or when only cost-tightness is attained, one may instead resort to a local solver and certify the solution candidate using Lagrangian duality. For completeness, we also mention that in some cases, one may extract a solution estimate from a higher-rank solution of the SDP in a procedure called ‘rounding’, see e.g., [5]. This typically consists of extracting the dominant eigenvector from \mathbf{X}^* , and projecting it to the feasible set of (1). Note that in this case there are no guarantees on the quality of the solution and cases have been reported where the obtained estimate is far from the global optimum [40].

We have seen that either rank- or cost-tightness are necessary for efficiently obtaining or certifying globally optimal solutions, respectively. The remaining question is how one may increase the tightness of a given problem. This leads to the notion of redundant constraints, as explained next.

D. Redundant Constraints

Redundant constraints can be added to (2) without changing its feasible set (thus the name ‘redundant’).⁵ While the constraints are redundant for the QCQP, they may, however, change the feasible region of the SDP. In particular, redundant constraints typically reimpose structure on \mathbf{X} that is lost when relaxing the rank-one constraint. For example, if the lifted vector is $\mathbf{x}^\top = [1 \ \theta \ \theta^2 \ \theta^3]$, then

$$\mathbf{X} = \mathbf{x} \mathbf{x}^\top = \begin{bmatrix} 1 & \theta & \theta^2 & \theta^3 \\ \star & \theta^2 & \theta^3 & \theta^4 \\ \star & \star & \theta^4 & \theta^5 \\ \star & \star & \star & \theta^6 \end{bmatrix}, \quad (10)$$

which has a very clear structure (it is a Hankel matrix, as is always the case for semidefinite relaxations of scalar polynomial problems [41]) that might be lost in the relaxation. The lifting constraints (in this case, $\mathbf{x}[3] = \mathbf{x}[2]^2$ and $\mathbf{x}[4] = \mathbf{x}[3]\mathbf{x}[2]$) and symmetry of the solution take care of constraining all terms of degree 0 to 3 as well as θ^5 , but nothing directly enforces that the elements corresponding to θ^4 in the variable \mathbf{X} are equal. In this case, we can add the redundant constraint corresponding to $(\mathbf{x}[3]^2 = \mathbf{x}[2]\mathbf{x}[4])$ to enforce exactly that. Redundant constraints can often be hard to find — as our continued example illustrates.

Example (stereo-1D, cont’d). *A simple computation shows that*

$$z_i - z_j = \frac{1}{\theta - a_i} - \frac{1}{\theta - a_j} = (a_i - a_j)z_i z_j, \quad (11)$$

which holds for any $i \neq j$ and z_i, z_j constructed using the lifting functions $\ell_i(\theta)$ introduced in (5). This shows that equation (11), which is quadratic in the elements of \mathbf{x} , is redundant in (2), but non-redundant in the QCQP. It can be added to the QCQP with matrices \mathbf{A}_{ij} ; $\mathbf{A}_{ij}[1, i] = \mathbf{A}_{ij}[i, 1] = 1$, $\mathbf{A}_{ij}[1, j] = \mathbf{A}_{ij}[j, 1] = -1$, $\mathbf{A}_{ij}[i, j] = \mathbf{A}_{ij}[j, i] = (a_i - a_j)$, for all $i, j \in [N], i \neq j$.

Because they impose more structure on \mathbf{X} , redundant constraints may have the effect of reducing the rank of \mathbf{X} , and thus improve the tightness of the relaxation. However, finding the right form and number of redundant constraints can be a tedious process, especially as the dimension of the problem increases. The present paper circumvents this process by proposing a numerical method to find all available redundant constraints, as we explain next.

IV. DETERMINING FEASIBILITY OF TIGHTENING (AUTOTIGHT)

In this Section, we present our method to determine whether a problem in a given form can be tightened, adding all possible redundant constraints without having to manually find or interpret them.

⁵Speaking in terms of algebraic geometry, the redundant constraints do not change the algebraic variety that is defined as the solution space.

⁴It is straightforward to see that rank-tightness implies cost-tightness.

A. Setting up the Nullspace Problem

At the core of the presented method is the idea that all of the constraint matrices \mathbf{A}_i lie in the nullspace of the linear subspace spanned by the feasible points. Indeed, assume we can generate feasible samples $\boldsymbol{\theta}^{(s)}$, and therefore also a set of lifted samples $\mathcal{X} = \{\mathbf{x}^{(1)}, \dots, \mathbf{x}^{(N_s)}\}$ with $\mathbf{x}^{(s)}$ constructed using the *known* lifting functions ℓ .⁶ Then, for any valid constraint \mathbf{A}_i (whether primary or redundant), we must have

$$\langle \mathbf{A}_i, \mathbf{X}^{(s)} \rangle = \text{vech}(\mathbf{A}_i)^\top \text{vech}(\mathbf{X}^{(s)}) = 0, \quad (12)$$

with $\mathbf{X}^{(s)} := \mathbf{x}^{(s)}\mathbf{x}^{(s)\top}$. This must hold for all samples $\mathbf{x}^{(s)}$. Defining the data matrix $\mathbf{Y} = [\text{vech}(\mathbf{X}^{(1)}) \dots \text{vech}(\mathbf{X}^{(N_s)})] \in \mathbb{R}^{n \times N_s}$, the set of ‘learned’ constraints, \mathcal{A}_l , is the left nullspace basis of \mathbf{Y} :

$$\mathcal{A}_l = \{\mathbf{A}_1, \dots, \mathbf{A}_{N_n}\} = \{\text{vech}^{-1}(\mathbf{a}_i) \mid \mathbf{a}_i^\top \mathbf{Y} = \mathbf{0}\}. \quad (13)$$

In other words, each nullspace basis vector corresponds to one (vectorized) constraint matrix. Therefore, finding all possible constraints is a standard nullspace problem. The dimension of the nullspace, N_n , corresponds to the total number of constraints. Note that we have exploited the fact that $\mathbf{X}^{(s)}$ and \mathbf{A}_i are symmetric in using the half-vectorization operator, which reduces the problem size to $n := \frac{N(N+1)}{2}$.

By definition, all the constraints found through (13) are linearly independent when operating in matrix form. When using the constraints in (6), however, the constraints may become dependent; in other words, the method finds both primary and redundant constraints.

Sometimes, it may be desirable to enforce some of the basis vectors to be known, for example to enforce the primary constraints. We denote the set of constraints to be enforced by $\tilde{\mathcal{A}}_k = \{\tilde{\mathbf{A}}_1, \dots, \tilde{\mathbf{A}}_{N_k}\}$. Completing the nullspace basis is as simple as appending the known constraints to the data matrix \mathbf{Y} :

$$\mathbf{Y} = [\text{vech}(\mathbf{X}^{(1)}) \dots \text{vech}(\mathbf{X}^{(N_s)}) \text{vech}(\tilde{\mathbf{A}}_1) \dots \text{vech}(\tilde{\mathbf{A}}_{N_k})]. \quad (14)$$

By definition, the left nullspace vectors of \mathbf{Y} will then be orthogonal to the known constraints.

To find a valid nullspace basis, we need to have at least $r = n - N_n$ samples, with n the number of rows of \mathbf{Y} , N_n the nullspace dimension, and r the rank of \mathbf{Y} . However, since r is not known a priori, a viable strategy is to randomly generate $N_s > n$ samples.⁷ This ensures that the data matrix is rank-deficient, and the nullspace basis can be calculated using the permuted QR decomposition, as we explain next.

B. Sparse Basis Retrieval

We know that the constraint matrices are typically sparse, since they usually involve a subset of variables. Can we

ensure that the learned constraints are expressed in a basis that encourages sparsity? Sparsity is good not only for lower runtime and memory consumption of SDP solvers, but also because sparser matrices are more easily interpretable, should we want to determine what the algebraic expression of the constraints is.⁸ Unfortunately, finding the sparsest nullspace basis is a NP-hard problem [42]. However, we can use a pivoted, or rank-revealing, QR decomposition [43] to find the left nullspace of the data matrix and to induce sparsity in the resulting basis vectors. We found the resulting constraints to be sufficiently sparse for downstream operations, and in both applications covered in Section VI, some basis vectors are even as sparse as analytically constructed constraints. Other matrix decomposition alternatives, such as the singular value decomposition (SVD), were empirically found to exhibit less sparsity.

The pivoted QR decomposition returns a decomposition of the form [43]

$$\mathbf{Y}^\top \mathbf{P} = \mathbf{Q}\mathbf{R} = \mathbf{Q} \begin{bmatrix} \mathbf{R}_1 & \mathbf{R}_2 \\ \mathbf{0} & \mathbf{0} \end{bmatrix}, \quad (15)$$

where \mathbf{P} is a $n \times n$ permutation matrix ensuring that the diagonal of \mathbf{R} is non-increasing, \mathbf{Q} is $N_s \times N_s$ and orthogonal, \mathbf{R}_1 is upper-diagonal with dimensions $r \times r$, and \mathbf{R}_2 is of size $r \times N_n$. The nullspace basis vectors \mathbf{a}_i are then given by

$$[\mathbf{a}_1 \dots \mathbf{a}_{N_n}] = \mathbf{P} \begin{bmatrix} \mathbf{R}_1^{-1} \mathbf{R}_2 \\ -\mathbf{I}_{N_n} \end{bmatrix}. \quad (16)$$

Note that when using the permuted QR decomposition, the obtained basis vectors are linearly independent, but not necessarily orthogonal to each other, as would be the case with an SVD, for example. However, we found that the increased sparsity was of higher importance, both for computational speed and interpretability, than orthogonality.

C. Determining Tightness

All considerations so far are independent of the cost function and only depend on the chosen substitutions and primary constraints. To determine if the relaxation is tight, we need to define the cost, *i.e.*, form the matrix \mathbf{Q} in (6). In general, tightness may be a function of both the noise magnitude [39] and the sparsity of the measurement graph [9]. The proposed method takes both into account as we fix \mathbf{Q} and then determine the tightness (and required redundant constraints) for this particular choice.

We determine cost-tightness by comparing the cost of the dual problem with the cost of a candidate global solution. The candidate global solution is found by running an off-the-shelf local solver initialized at the ground-truth state, which we expect to be close to the optimal solution for low-enough noise. Indeed, this strategy allowed us to find the global minimum almost always for the noise regimes considered in Section VI. If not, we regenerate a new random setup and start again.⁹ We compute the relative duality gap (RDG) between

⁶Note that we can also allow for unknown or numerical lifting functions, as long as a sampler of \mathbf{x} is available.

⁷The emphasis here is on random; this ensures that all samples are linearly independent with probability one, to yield what is also called ‘generic’ samples [18]. Intuitively speaking, when using generic samples one can ensure that properties derived from the samples hold for the entire variety.

⁸We reiterate that interpretability is not necessary, but it may be beneficial for scalability and for gaining a better understanding of a given problem.

⁹As soon as we find that the cost of the candidate solution is equal to the dual cost (up to numerical tolerance), we know that it corresponds to the global minimum, because of duality theory [11].

the cost of this local solution, called \hat{q} , and the optimal dual cost d^* through $(\hat{q} - d^*)/q^*$, and report cost-tightness if the RDG is below a fixed threshold (see Section VI-A).

To determine rank-tightness, we calculate the eigenvalues of the solution \mathbf{X} , and take the ratio of the first to the second-largest eigenvalue, called the singular-value ratio (SVR) in what follows. If the ratio is larger than a fixed value (see Section VI-A) we report that the solution is rank one.

D. Summary

We conceptualize the algorithm AUTOTIGHT, which is defined by the successive application of IV-A to IV-C, by the gray boxes in Figure 2. In summary, we randomly generate $N_s > n$ samples of the half-vectorized feasible points and compute a nullspace basis of the samples, which gives us all possible constraints. We then determine if the SDP relaxation is rank- or cost-tight when using all found constraints. There are three possible outcomes of this method:

- 1) The problem cannot be tightened. Knowing this, no additional effort has to be spent in trying to find redundant constraints for this formulation. Either a new formulation can be tried — adding for instance (a subset of) higher-order Lasserre terms [13] — or the SDP can be used in conjunction with rounding, for example as an initialization for a local solver.
- 2) The problem can be tightened without any redundant constraints, or with few redundant constraints that are interpretable. By interpretable we mean that the algebraic form can be derived directly from each matrix — we will see such examples in Section VI, Figure 4. In this case, constraints matrices can be efficiently created analytically, as in classical methods [7].
- 3) The problem can be tightened, but with many redundant constraints. In this case, the method presented so far would have to be reapplied to any new problem instance in order to find the required redundant constraints, which does not scale to the large problem sizes typically encountered in robotics.

We will revisit the first two outcomes in the experiments in Section VI. The next section deals with the third outcome: We present a method that finds what we call *constraint templates* — particular patterns that can be applied to any number and combination of variables of particular types.

V. GENERATING SCALABLE CONSTRAINTS (AUTOTEMPLATE)

The method AUTOTIGHT finds, for a given problem instance, whether the problem can be tightened. However, tightness will most likely be lost as we increase the problem size if we do not add the redundant constraints corresponding to new variables. Applying AUTOTIGHT is prohibitively expensive as the dimensionality of the problem increases, due to the cubic complexity of the QR decomposition. We thus present AUTOTEMPLATE, an extended version of AUTOTIGHT that is more scalable.

A. Algorithm Overview

Thankfully, while problems in robotics tend to be high-dimensional, they usually only exhibit a few different variable types. For example, in SLAM, the only variable types are robot poses and landmark positions [2]. We would expect the constraints relating instances from the same variable types to be repeatable; for example, all constraints that touch one pose should hold for all other poses too.

The additions to AUTOTIGHT to make it scalable are shown in the white and dashed boxes in Figure 2. Initially, we still operate on a small example problem; however, the output of AUTOTEMPLATE are templates that can be scaled to any problem size. The method consists of the following steps:

- 1) We set up the nullspace problem as explained in IV-A, but now we only operate on one variable group at a time, which leads to much smaller nullspace problems. At this point, we may also factor out parameters — variables of our problem that are known a priori, such as landmark positions in localization problems. We explain this in more detail in V-B.
- 2) We compute the nullspace vectors as in Section IV-B, but interpret the resulting basis vectors as constraint templates.
- 3) We apply these templates to all other variables of the same group(s) as outlined in V-C.
- 4) We check tightness of the problem as in Section IV-C. If the problem is tight, we return all the learned constraints as templates. If it is not, we go back to step 1).

As opposed to AUTOTIGHT, AUTOTEMPLATE requires some manual input by the user: defining the variable groups and parameters, and their order of consideration. Compared to having to manually find and define required redundant constraints, this is relatively simple. We give examples of variable selections for the examples studied in this paper in Table II in Section VI, which likely extend to most problems encountered in robotics.

B. Factoring Out Parameters

For some problems, constraints may depend on parameters that are known a priori. In the stereo-1D example presented in Section III, and in the stereo-based localization problem presented in Section VI-C, for example, the constraints depend on the known landmark coordinates. Because of this, the learned constraints may not be applicable to other random setups. To overcome this problem, we treat such quantities as ‘parameters’ and append them to the samples of feasible points. Let $\mathbf{p} \in \mathbb{R}^{N_p}$ be the vector of N_p parameters, for instance the coordinates of landmarks, and let $\kappa(\mathbf{p}) : \mathbb{R}^{N_p} \rightarrow \mathbb{R}^K$ be a chosen lifting function that outputs K lifted elements. This lifting function needs to be chosen generally enough so that it encompasses all expected dependencies. In the absence of prior knowledge, we suggest monomials up to the maximum degree of θ in (2). For example, for up to quadratic substitutions we would use

$$\kappa(\mathbf{p}) = \text{vech} \left(\begin{bmatrix} 1 \\ \mathbf{p} \end{bmatrix} \begin{bmatrix} 1 & \mathbf{p}^\top \end{bmatrix} \right). \quad (17)$$

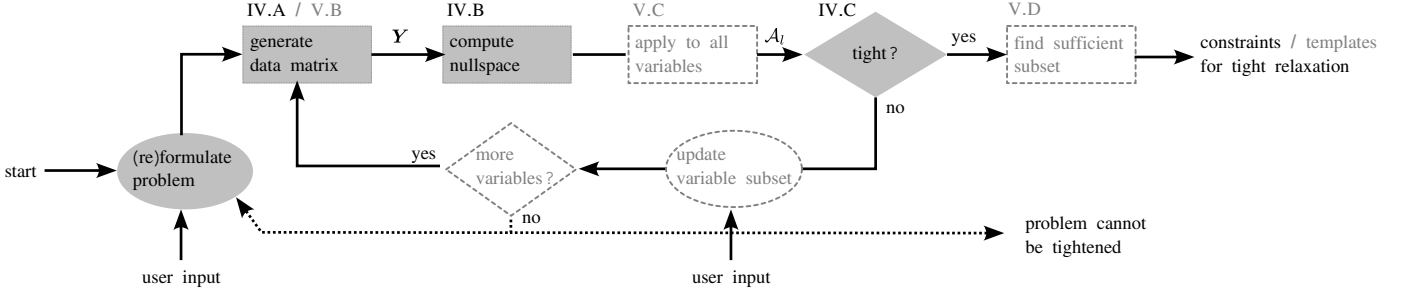


Fig. 2: Overview of proposed algorithm to automatically find constraints or templates. Highlighted in gray and white, respectively, are the components of AUTOTIGHT and AUTOTEMPLATE. The two stages where (minor) user input is required are shown in the bottom.

Using the lifted parameters, we modify each feasible sample to include the parameter dependencies, leading to the ‘augmented’ feasible sample $\bar{z}^{(s)} \in \mathbb{R}^{\bar{n}}$ of size $\bar{n} := nK$:

$$\bar{z}^{(s)} := \text{vech} \left(\mathbf{x}^{(s)} \mathbf{x}^{(s)\top} \right) \otimes \kappa(\mathbf{p}). \quad (18)$$

The augmented data matrix $\bar{\mathbf{Y}} \in \mathbb{R}^{\bar{n} \times \bar{N}_s}$ is given by

$$\bar{\mathbf{Y}} = [\bar{\mathbf{z}}_1 \quad \cdots \quad \bar{\mathbf{z}}_{\bar{N}_s}], \quad (19)$$

where we note that the number of samples \bar{N}_s now has to be chosen as to ensure that $\bar{\mathbf{Y}}$ is rank-deficient. We denote the left nullspace basis vectors of (19) by $\bar{\mathbf{a}}_l \in \mathbb{R}^{\bar{n}K}$, with $l \in [\bar{N}_n]$. We call these basis vectors ‘templates’ because we will apply them to new variable sets, and in particular, scale them to any required problem size, as we explain next.

C. Applying Templates

Conceptually speaking, applying the templates means repeating each constraint for each possible combination of the variables that it involves. For example, if one constraint matrix involves one position and two different landmarks, then we repeat the constraint for each position and each possible pair of landmarks per position. To facilitate this operation programmatically, we have created an easy-to-use tool to generate sparse matrices using variable names for indexing.¹⁰ That way, applying constraints to all possible variables simply means creating duplicates of a given constraint, and then renaming the variables that it touches.

If parameters were factored out as explained in V-B, then they need to be factored back in before solving the SDP, using the current parameter realization. We introduce the operator $\text{mat}(\cdot)$, which folds the augmented basis vector $\bar{\mathbf{a}}_l$ (which we recall has nK dimensions, with K the number of lifted parameters) column-wise into a $n \times K$ matrix. Then, *factoring in* the parameters of a specific parameter realization $\mathbf{p}^{(s)}$ can be written as

$$\mathbf{a}_l = \text{mat}(\bar{\mathbf{a}}_l) \kappa(\mathbf{p}^{(s)}), \quad (20)$$

where the output $\mathbf{a}_l \in \mathbb{R}^n$ is now a problem-specific vectorized constraint that can be converted to the corresponding constraint matrix $\mathbf{A}_l = \text{vech}^{-1}(\mathbf{a}_l)$. We return to the stereo-1D example to illustrate these concepts:

Example (stereo-1D, cont’d). Looking at (11), we see that the redundant constraints depend on the problem parameters \mathbf{a}_i : we have $\mathbf{p}^\top := [a_1 \cdots a_N] \in \mathbb{R}^N$ and $K := N$. Because the lifting constraints $l_i(\mathbf{x})$ are linear in θ , we introduce the lifting function $\kappa(\mathbf{p}) := [1 \ a_1 \ a_2 \ \cdots \ a_N]^\top$. We define the following set of variable groups: $\{(1, \theta, z_1, a_1), (1, \theta, z_1, a_1, z_2, a_2), \dots\}$. When imposing the known substitution constraints, we would not find any additional constraints at the first level. At the second level, however, each augmented sample would be of the form:

$$\bar{\mathbf{z}}^\top := [1 \ \theta \ z_1 \ z_2 \ \theta^2 \ \theta z_1 \ \theta z_2 \ z_1^2 \ z_1 z_2 \ z_2^2] \otimes [1 \ a_1 \ a_2], \quad (21)$$

where we have dropped superscript (s) for better readability. Clearly, the redundant constraints would now be in the nullspace of the augmented data matrix, as we have:

$$0 = \bar{\mathbf{a}}_1^\top \bar{\mathbf{z}} = [\alpha_1^\top \ \alpha_2^\top \ \alpha_3^\top] \bar{\mathbf{z}}, \quad (22)$$

for any $\bar{\mathbf{z}}$, where we have introduced

$$\begin{aligned} \alpha_1^\top &= [0 \ 0 \ 1 \ -1 \ 0 \ 0 \ 0 \ 0 \ 0 \ 0], \\ \alpha_2^\top &= [0 \ 0 \ 0 \ 0 \ 0 \ 0 \ 0 \ 0 \ 1 \ 0], \\ \alpha_3^\top &= [0 \ 0 \ 0 \ 0 \ 0 \ 0 \ 0 \ 0 \ 0 \ -1]. \end{aligned} \quad (23)$$

Note that the template $\bar{\mathbf{a}}_1$ does not depend on the landmarks anymore. This template can be applied to any variables by changing the labels as explained in Section V-C. Given also new realizations of parameters $\mathbf{p}^{(t)}$ corresponding to the new variables, we can create the corresponding constraint matrix:

$$\begin{aligned} \mathbf{a}_1^{(t)} &= \text{mat}(\bar{\mathbf{a}}_1) \mathbf{p}^{(t)} = [\alpha_1 \ \alpha_2 \ \alpha_3] \begin{bmatrix} 1 \\ a_1^{(t)} \\ a_2^{(t)} \end{bmatrix}, \\ \mathbf{A}_1^{(t)} &= \text{vech}^{-1}(\mathbf{a}_1^{(t)}). \end{aligned} \quad (24)$$

D. Reducing the Number of Constraints

Even when using the efficient sparse representation, applying the templates to all other possible combinations of variables can become the computational bottleneck of the problem. However, in practice not all of the found templates are actually necessary for tightness. Therefore, we suggest to prune the found templates before applying them to large problem sizes. In order to do that, we proceed as follows.

¹⁰The code is available as an open-source package at https://github.com/utiasASRL/poly_matrix.

Assume we have found a set of learned constraints \mathcal{A}_l for which the problem is (at least) cost-tight. Then, we can solve the following optimization problem in an attempt to sort the constraints by their importance for tightness:

$$\begin{aligned} & \min_{\lambda, \rho} \|\lambda\|_1 \\ \text{s.t. } & \mathbf{H}(\rho, \lambda) \succeq 0 \\ & \mathbf{H}(\rho, \lambda) \hat{\mathbf{x}} = \mathbf{0}, \end{aligned} \quad (25)$$

where $\|\cdot\|_1$ denotes the L_1 -norm, \mathbf{H} is defined as in (8) (with the learned matrices substituted for \mathbf{A}_k) and $\hat{\mathbf{x}}$ is the optimal solution of (6), found as explained in IV-C. Intuitively, Problem (25) finds a sparse set of dual variables required for cost-tightness, as the L_1 -norm promotes sparsity. By ordering the learned constraints by decreasing magnitude of λ and adding them one by one, we find which subset of constraints is sufficient for cost-tightness. This problem naturally lends itself to a bisection-like algorithm, where we try using all and no redundant constraints, at first, and then continue trying cutting the number of constraints in half. We terminate when the considered interval is of size one. At that point, we use only these constraints as templates, which significantly reduces the computation cost of all downstream operations, as shown in Section VI.

As another pruning step, we also make sure that all constraints are linearly independent after applying templates to other variables. For this purpose, we use the same rank-revealing QR decomposition as in IV-B but keep only the valid range-space basis vectors. Because of the sparsity of the constraints, this adds no significant cost.

E. Summary

To summarize, AUTOTEMPLATE generates scalable templates by iteratively finding the nullspace basis of smaller subsets of variable groups. We stop when the templates lead to a tight relaxation after applying them to all variable groups in a given example problem. Then, we find a subset of constraints sufficient for tightness, which can be used as templates for any new problem of the same type. When constraints depend on problem parameters, such as landmark coordinates, we also suggest a method to factor out this dependency and learn ‘augmented’ templates instead.

VI. EXPERIMENTAL RESULTS

We show the effectiveness of the proposed method on a variety of robotics problems encountered in real-world applications. First, we provide an in-depth analysis of two example applications, providing new insights on the tightness of their relaxations. The first application is range-only localization with fixed and known landmarks, such as encountered in ultra-wideband (UWB)-based localization [44, 45] or WiFi- or Bluetooth-based indoor localization [46]. We evaluate two different formulations, one of which requires redundant constraints while the other one does not. In this example, we find constraints are interpretable and we can derive their algebraic expressions.

TABLE I: Overview of the considered problems, their tightness and whether they require redundant constraints. Highlighted in red are formulations that were found to be non-tight.

Problem	lifting function	redundant constr.	cost-tight	rank-tight
range-only localization	\mathbf{z}	no	yes	yes
	\mathbf{y}	yes	yes	yes
stereo pose estimation	\mathbf{u}	yes	no	no
	$\mathbf{u}, \mathbf{u} \otimes \mathbf{t}$	yes	yes	no
point-point registration [10] (PPR)	none	no	yes	yes
point-line registration [10] (PLR)	none	yes	yes	yes
robust point-cloud registration [7] (rPPR)	$\boldsymbol{\theta} \otimes \boldsymbol{\theta}$	yes	no	no
	$\boldsymbol{\theta} \otimes \mathbf{w}$	yes	yes	no
robust absolute pose estimation [7] (rPLR)	$\boldsymbol{\theta} \otimes \boldsymbol{\theta}$	yes	no	no
	$\boldsymbol{\theta} \otimes \mathbf{w}$	yes	yes	no

The second application is stereo-based pose estimation using the reprojection error, which incorporates the realistic scenario of noise in pixel space [47]. To the best of our knowledge, this problem has not been successfully relaxed to a tight SDP before, with common solutions typically resorting to the back-projection error [48, 16], where the error is assumed Gaussian in Euclidean space instead. Closest to our solution is [19], where a branch-and-bound method in combination with a (non-tight) semidefinite relaxation is used to minimize the reprojection cost. Instead, we use our proposed method to find a formulation of the problem that can be tightened, with a significant number of redundant constraints that we automatically determine. These constraints scale poorly with problem size, are not interpretable, and depend on the problem parameters (known landmarks). Therefore, the second part of our proposed method is essential in this case.

Finally, we select representative examples from multimodal registration [10] and robust estimation [7], and verify their tightness results using our method. An overview of all problems considered in this Section is given in Table I.

A. Hyperparameters

Throughout the experiments, we keep the following parameters fixed. When learning the constraints, we oversample the data matrix \mathbf{Y} by 20% to improve conditioning of the nullspace problem.

For the SDP solver, we use MOSEK [38] interfaced through `cvxpy` [49, 50], fixing the tolerances of primal and dual feasibility, as well as the relative complementary gap to 10^{-10} and the tolerance of infeasibility to 10^{-12} . For finding the minimal set of constraints (Section V-D), we set the relative gap termination to 10^{-1} to allow even for inaccurate solutions to be returned (as the output is only used for ordering the constraints). We input the problems in dual form and set the MOSEK form to dual, meaning the primal formulation is actually solved. All other parameters are set to default.

For the local solver, we use the off-the-shelf `pymanopt` [51] solver, using the conjugate gradient optimizer and default stopping criteria (10^{-6} in gradient

norm and 10^{-10} in step size). When inequality constraints are present in the QCQP, we use the log-sum-exp function described in [52, §4.1] with $\rho = 10$ and $u = 10^{-3}$. For the range-only and the stereo-based localization problem, we use the `scipy` implementation of the BFGS solver, and our custom GN implementation, respectively, with the same stopping criteria as for `pymanopt`.

A problem is considered cost-tight when its RDG is below 1%. It is considered rank-tight when the SVR is above 10^7 .

Parameters that change for each problem, such as the considered noise levels, variable groups, and toy problem sizes, are summarized in Table II. We use fully-connected measurement graphs for all considered problems.¹¹

B. Range-Only Localization

1) *Problem Statement:* The goal of range-only (RO) localization is to estimate the position of a moving device over time, given range measurements to fixed and known anchors. We call the anchor points $\mathbf{m}_k \in \mathbb{R}^d$ with $k \in [N_m]$ and the position at time t_n is denoted $\boldsymbol{\theta}_n \in \mathbb{R}^d$, with $n \in [N]$. We use $d = 3$ in all of the experiments. One commonly used formulation of the problem is [40]

$$\min_{\boldsymbol{\theta} \in \mathbb{R}^{Nd}} \sum_{n,k \in \mathcal{E}} \left(d_{nk}^2 - \|\mathbf{m}_k - \boldsymbol{\theta}_n\|^2 \right)^2, \quad (26)$$

where $\boldsymbol{\theta} \in \mathbb{R}^{Nd}$ contains the stacked position variables and \mathcal{E} is the edge set of a measurement graph, with an edge between position n and anchor k if that distance d_{nk} has been measured. Note that it is straight-forward to include a motion prior in (26), such as a constant-velocity prior, as shown in [34]. Such priors are typically up to quadratic in the unknowns, thus not requiring any special treatment when it comes to constraints, and are omitted for simplicity.

Problem (26) is quartic in the unknowns, and thus may contain multiple local minima [34]. However, by introducing substitutions that are quadratic in $\boldsymbol{\theta}_n$, it can be lifted to a QCQP, making it a candidate for SDP relaxation. We study two different substitutions. First, looking at the cost of (26), we see that the substitution

$$z_n := \|\boldsymbol{\theta}_n\|^2 \in \mathbb{R} \quad (27)$$

is enough to make the problem quadratic in the lifted vector $\mathbf{x}^\top = [1 \ \boldsymbol{\theta}_n^\top \ z_n]$. This is in fact the substitution that was used in [34] and was shown to require no redundant constraints for tightness.¹² Here, we also study the more methodological substitution that introduces all quadratic terms of $\boldsymbol{\theta}_n$, or in other words:

$$\mathbf{y}_n := \text{vech}(\boldsymbol{\theta}_n \boldsymbol{\theta}_n^\top) \in \mathbb{R}^{d(d+1)/2}. \quad (28)$$

2) Determining Feasibility of Tightening (AUTOTIGHT):

We start by using AUTOTIGHT to evaluate the two different substitutions, using the small example problem, defined in Table II.

¹¹This means that we assume that at each pose, all landmarks are measured.

¹²The substitution (28) can be categorized as a ‘sparse Lasserre’ [17] substitution, as not all individual quadratic terms are added.

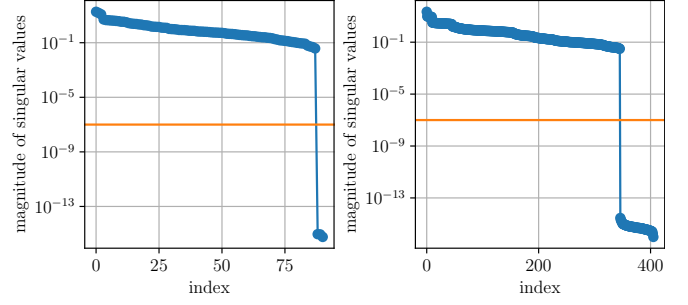


Fig. 3: Singular value spectrum of the data matrix for RO localization. The singular values below the threshold (in orange) correspond to the nullspace basis vectors. For the substitution z_n (27) (left plot), we find 3 basis vectors, however, for the substitution \mathbf{y}_n (28) (right plot) we find 20 basis vectors.

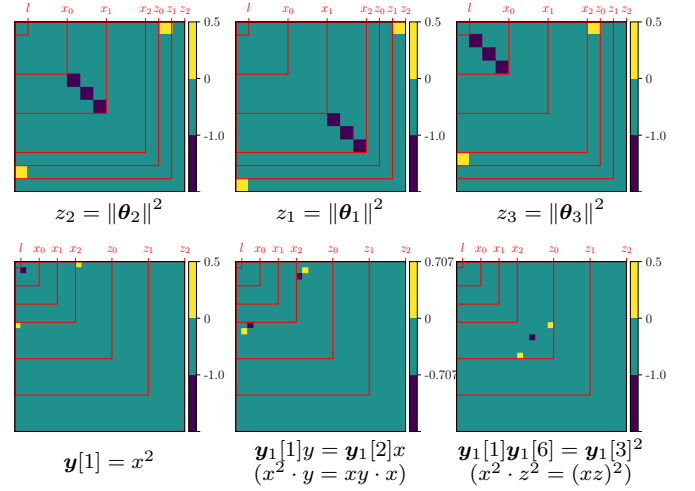


Fig. 4: Examples of learned constraint matrices for z_n substitution (top) and the \mathbf{y}_n substitution (bottom) of RO localization. Shown above each matrix are the algebraic identities that the matrices enforce. For simplicity, we call $\boldsymbol{\theta}_1^\top = [x \ y \ z]$.

The data matrix for both substitutions exhibits a well-separated nullspace, as can be seen in Figure 3. We can see immediately that the z_n substitution leads to a small nullspace ($N_n = 3 = N$), corresponding exactly to the number of substitutions.¹³ The substitution \mathbf{y}_n , on the other hand, leads to a nullspace that includes more than just the substitution variables ($N_n = 60 = 20N$), which shows the existence of redundant constraints.

We show the three found constraint matrices for the z_n substitution in the first row of Figure 4. Surprisingly, the three automatically found matrices correspond exactly to the three substitution formulas (shown below each matrix). The second row of Figure 4 shows three example matrices for the \mathbf{y}_n substitution. The first one is an example of a substitution constraint found by the algorithm, while the other two matrices are examples of discovered redundant constraints. Our method finds the $d(d+1)/2 = 6$ substitution constraints, and 14 redundant constraints similar to the two shown examples. For completeness, Figure 5 shows a compact representation of

¹³We chose not to enforce the known constraint matrices, to point out the interpretability of the found constraints.

TABLE II: Overview of the tightened problems, including the variable groups, problem dimensions, and noise parameters. For simplicity, all substitutions are called z_i . N_{out} denotes the number of outliers, and noise levels correspond to the standard deviation of zero-mean Gaussian noise.

Problem	Parameters	Variables	Inlier noise (Outlier noise)
range-only localization	$d = 3, N_m = 10, N = 3$	$\{\{h, \theta_0\}, \{h, z_0\}, \{h, \theta_0, z_0\}, \dots\}$	10^{-2}
stereo-localization	$d \in \{2, 3\}, N = d + 1$	$\{\{h, \theta\}, \{h, z_0\}, \{h, \theta, z_0\}, \{h, z_0, z_1\}, \dots\}$	1.0
point-point registration [10]	$d = 3, N = 3$	$\{\{h, \theta\}\}$	10^{-2}
point-line registration [10]	$d = 3, N = 5$		10^{-3}
robust point-cloud registration [7]	$d = 3, N = 4, N_{\text{out}} = 1$	$\{\{h, \theta\}, \{h, \theta, w_0\}, \{h, \theta, z_0\}, \{h, \theta, w_0, w_1\}\}$	10^{-2} (1.0)
robust absolute pose estimation [7]	$d = 3, N = 6, N_{\text{out}} = 1$	$\{h, \theta, w_0, z_0\}, \{h, \theta, z_0, z_1\}, \dots\}$	10^{-3} (0.1)

TABLE III: Breakdown of characteristics for all tightened problems for the first stage of AUTOTEMPLATE. This stage has to be run only once, as the output are constraint templates. All times are in seconds, with t_n the total time to compute the nullspaces, t_a the time to apply templates to all variables, t_s the time to check for tightness, and t_r the time required to reduce the constraints using (25).

Problem	Dimensions n per iteration	# Constraints	# Sufficient	t_n	t_a	t_s	t_r	Total time	RDG	SVR
RO (z_n)	15	3	3	0.01	0.01	0.30	0.15	0.46	7.05e-06	1.76e+09
RO (y_n)	55	60	38	0.14	0.07	0.24	0.51	0.97	4.29e-06	2.29e+09
stereo (2d)	28 168 546 1365	170	36	4.74	0.31	0.48	4.26	9.79	5.49e-05	4.75e+00
stereo (3d)	91 910 3250 9100	638	107	267.01	1.15	1.65	18.91	288.72	6.95e-06	2.10e+01
PPR	91	20	8	0.17	0.03	0.26	0.26	0.72	4.39e-06	3.88e+07
PPL	91	20	10	0.17	0.03	0.36	0.31	0.86	4.46e-05	1.47e+07
rPPR	91 105 325 120 351 703	1232	506	6.30	2.88	5.80	78.96	93.93	3.47e-10	2.82e+01
rPLR	91 105 325 120 351 703	2294	1894	6.49	5.06	9.83	359.88	381.26	3.81e-05	1.54e+01

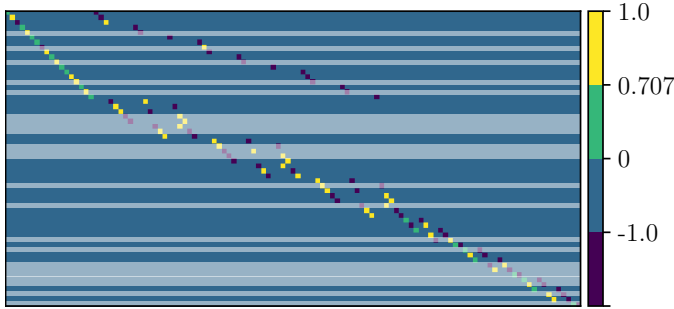


Fig. 5: Compact visualization of the learned constraint matrices for the y_n substitution of RO localization. Each row contains one basis vector, equivalent to the half-vectorized constraint matrix. Highlighted in dark are the sufficient constraints for rank-tightness.

all the constraints for the y_n substitution, where each row corresponds to one found basis vector (the constraint matrix in half-vectorized form). We can see that all learned matrices are sparse and quantized, with nonzero values in $\{-1, \frac{1}{\sqrt{2}}, 1\}$.

We find that both substitutions lead to cost-tight and rank-tight relaxations when all constraints are imposed, as shown in Table III. For the y_n substitution, redundant constraints are required. Exactly what constraints are required and how they scale is investigated next.

3) Generating Scalable Constraints (AUTOTEMPLATE):

We have shown that the formulations with substitution y of the RO localization problem can be tightened, at least for a small problem. In this section, we show that the method can be generalized to problems of larger size. In this particular example, the learned constraints are interpretable, therefore we could infer the mathematical expression of all constraints, as we saw in Figure 4, and apply them to new setups; we are thus in outcome 2) of Section IV-D. Instead, we show here that the algorithmic way of scaling up, which does not require any

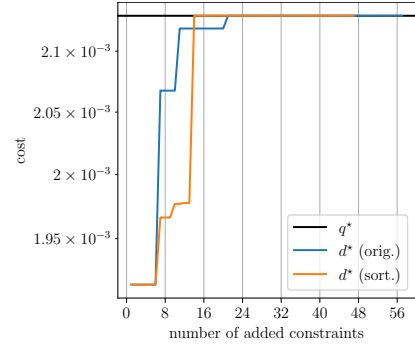


Fig. 6: Cost-tightness for RO localization, using the y_n substitution. We compare the cost of the dual problem (colored curves) to the cost of the original QCQP (black horizontal line), as we add the constraints in the order output by the QR decomposition (blue) vs. the order dictated by the method in Section V-D.

intermediate manual steps, is also tractable for larger problem sizes.

To generate scalable templates, we use AUTOTEMPLATE. We still use $N = 3$ positions, and alternate adding one new position and one new substitution at a time, as shown in Table II. The algorithm terminates after including variables, $\{h, \theta_0, y_0\}$, at which point the found templates lead to a tight relaxation (in both cost and rank) when applied to all $N = 3$ positions.¹⁴

Before applying the templates to new problems of increasing size, we reduce them to a sufficient subset of constraints as explained in Section V-D. Figure 6 shows the evolution of the dual cost vs. the QCQP cost (i.e., cost-tightness) as more

¹⁴Note that we do not need to consider any combinations of positions (or substitutions), which is a consequence of the problem being separable. This could have been observed from (26), but we did not exploit this structure here to make as few assumptions as possible.

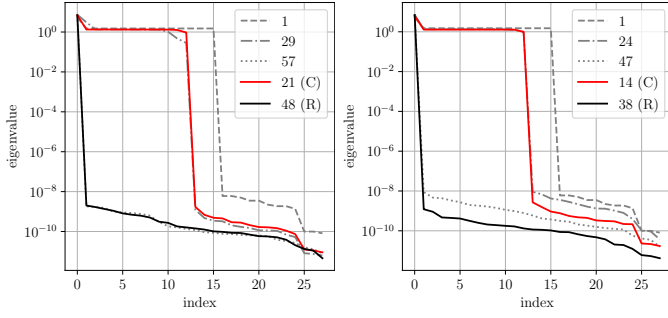


Fig. 7: Study of eigenvalue spectra for \mathbf{y}_n substitution, using the original constraint order (left) the order sorted by (25) (right). We compare the spectra as more constraints are added (gray lines), highlighting the points where cost-tightness (C) and rank-tightness (R) are obtained in red and black, respectively.

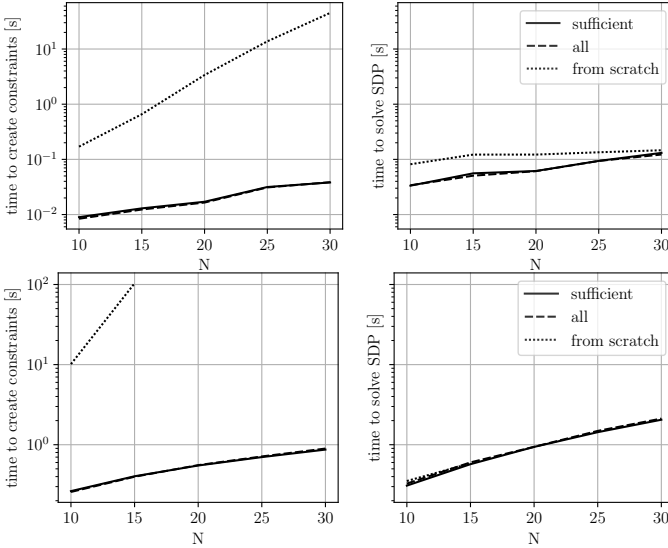


Fig. 8: Timing study for RO localization, using the \mathbf{z}_n substitution (top) vs. the \mathbf{y}_n substitution (bottom). We compare using only the sufficient (solid line) or all templates (dashed line) output by AUTOTEMPLATE, which are very close for this particular problem. They compare favorably to learning constraints from scratch for each problem using AUTOTIGHT.

constraints are added. When using the ordering as output by the QR decomposition, tightness is achieved after adding a total of 21 constraints (including homogenization). On the other hand, when adding the constraints in the order dictated by the sparsity-promoting SDP (25), cost-tightness is attained after adding only 14 constraints. Figure 7 shows the evolution of rank-tightness for different orders for the \mathbf{y}_n substitution. As expected, more redundant constraints are required for rank-tightness than for cost-tightness: 48 when using the original order vs. 38 when using the sorted matrices.

We generalize the found templates to problems with up to 30 positions. Figure 8 shows the time required for creating the constraints and solving the SDP for each problem size. We compare the processing times of learning the constraints for each problem from scratch using AUTOTIGHT, with using templates computed from AUTOTEMPLATE, using either all or only those sufficient for rank-tightness. Naturally, when using the substitution \mathbf{z}_n , applying templates and checking for

tightness remain relatively cheap as the problem size grows, because the number of total constraints grows only linearly in the number of variables. Even learning the constraints from scratch is reasonably fast for this case. For the substitution \mathbf{y}_n , however, AUTOTIGHT becomes prohibitively expensive beyond $N = 15$ positions. On the other hand, when using only the subset of sufficient constraints, the cost of generating the constraints is close to the cost of solving the SDP for all problem sizes. Solving the SDP is only slightly faster when using only the sufficient constraints as templates, because in this example, the numbers of constraints are not significantly different. Note that learning the templates and determining the sufficient subset constitute a fixed cost and are listed separately in Table III.

C. Stereo-Based Localization

1) *Problem Statement:* In stereo localization, the goal is to estimate a stereo camera's pose given the image coordinates, in both left and right frames, of a number of known landmarks. In analogy with range-only localization, we call the known, homogenized landmarks \mathbf{m}_k with $k \in [N_m]$. For simplicity, we focus on one measurement time only, and call the unknown pose at that time $\mathbf{T} \in SE(d)$, which contains both the rotation matrix from world to camera frame, $\mathbf{C} \in SO(d)$, and the associated translation $\mathbf{t} \in \mathbb{R}^d$. We collect the pixel measurements of landmark k in $\mathbf{y}_k^\top := [u_k^{(l)} \ v_k^{(l)} \ u_k^{(r)} \ v_k^{(r)}]$, where u and v denote the x and y coordinates in pixel space, and superscripts (l) and (r) correspond to the left and right frame, respectively. We call the intrinsic stereo camera matrix in d dimensions \mathbf{M}_d , with

$$\mathbf{M}_2 = \begin{bmatrix} f_u & c_u & f_u \frac{b}{2} \\ f_u & c_u & -f_u \frac{b}{2} \end{bmatrix}, \quad \mathbf{M}_3 = \begin{bmatrix} f_u & 0 & c_u & f_u \frac{b}{2} \\ f_v & c_v & 0 & 0 \\ f_u & 0 & c_u & -f_u \frac{b}{2} \\ f_v & c_v & 0 & 0 \end{bmatrix}, \quad (29)$$

and f_u , f_v , and b are the focal lengths and baseline, respectively. Then, the forward measurement model is given by:

$$\mathbf{y}_k = \mathbf{M} (\mathbf{e}_d^\top \mathbf{T} \mathbf{m}_k)^{-1} \mathbf{T} \mathbf{m}_k, \quad (30)$$

where \mathbf{e}_d is the d -th standard basis vector. Given a number of pixel measurements from N landmarks, the pose can be estimated as the solution of the optimization problem

$$\min_{\mathbf{T} \in SE(d)} \sum_{k \in [N]} \|\mathbf{y}_k - \mathbf{M} (\mathbf{e}_d^\top \mathbf{T} \mathbf{m}_k)^{-1} \mathbf{T} \mathbf{m}_k\|^2. \quad (31)$$

Due to the $SE(d)$ constraint and the rational cost function, Problem (31) is hard to solve globally. However, the problem can again be lifted to a QCQP by introducing a series of relaxations and substitutions. First, we relax the $SO(d)$ to a $O(d)$ constraint, which essentially drops the $\det(\mathbf{C}) = 1$ constraint. As discussed in [5], this relaxation is often tight without additional constraints, and if not, handedness constraints can be added [10]. As we are automatically finding all redundant constraints, this constraint will be added later if required. Secondly, we can introduce the substitution $\mathbf{v}_k := (\mathbf{e}_d^\top \mathbf{T} \mathbf{m}_k)^{-1} \mathbf{T} \mathbf{m}_k$, which can be written as a quadratic

constraint by multiplying both sides with the denominator. This yields the following QCQP:

$$\begin{aligned} \min_{\mathbf{C}, \mathbf{t}} \quad & \sum_{k \in [N]} \|\mathbf{y}_k - \mathbf{M} \mathbf{v}_k\|^2 \\ \text{s.t.} \quad & (\mathbf{I}_d - \mathbf{v}_k \mathbf{e}_d^\top) \mathbf{T} \mathbf{m}_k = \mathbf{0}, k \in [N] \\ & \mathbf{C}^\top \mathbf{C} = \mathbf{I}_d. \end{aligned} \quad (32)$$

In order to write the above as a homogeneous QCQP, we introduce the lifted vector $\mathbf{x} \in \mathbb{R}^{N_x}$, with $N_x = 1 + \frac{d(d+1)}{2} + (1+N)d$ and

$$\mathbf{x}^\top = \begin{bmatrix} h & \text{vec}(\mathbf{C})^\top & \mathbf{t}^\top & \mathbf{u}_1^\top & \cdots & \mathbf{u}_N^\top \end{bmatrix}, \quad (33)$$

where \mathbf{u}_k is obtained by removing the d -th element of \mathbf{v}_k , which is always one by definition.

2) Determining Feasibility of Tightening (AUTOTIGHT):

As before, we first use AUTOTIGHT to investigate whether Problem (32) can be tightened. We use a small toy problem, choosing $N = d + 1$ landmarks. This problem is significantly higher-dimensional than the range-only problem, as a consequence of the orientation variable (with d^2 elements when using the orientation matrix representation) and the higher-dimensional substitutions (with d elements per landmark).

The left plots of Figure 10 show the cost-tightness study for a 2D problem and 3D problem. Even when adding all possible constraint matrices (34 of them in 2D and 43 in 3D), the problem cannot be tightened in the present form. Note how quickly we came to this conclusion: no manual search for redundant constraints had to be performed, a process that can be very time consuming.

We resort to (sparse) Lasserre's hierarchy [13] to tighten the problem. We proceed by trying different higher-order lifting functions and retesting for tightness after adding all possible redundant constraints. We individually test additions such as $\mathbf{u}_k \otimes \mathbf{u}_k$, $\mathbf{t} \otimes \mathbf{t}$, etc. and find that by adding $(\mathbf{u}_k \otimes \mathbf{t})$ to each landmark, we achieve tightness. For simplicity, we call the combined substitution $\mathbf{z}_k^\top := [\mathbf{u}_k^\top \quad (\mathbf{u}_k \otimes \mathbf{t})^\top] \in \mathbb{R}^{d+d^2}$. Figure 10 on the right shows the now-passing cost-tightness tests for 2D and 3D. Since cost-tightness is achieved, we can solve (25) to determine a smaller subset of sufficient constraints, which significantly reduces the number of sufficient constraints from 170 to 36 in 2D and from 638 to 107 in 3D, as shown in Figure 10 and Table III. In all considered cases, rank-tightness is not attained (see Figure 9) and may require additional lifting functions of even higher order. As we are already approaching what is computationally feasible for the SDP solver, we settle for cost-tightness for now.

A comparison of the accumulated sparsity patterns (i.e., the element-wise-or mask of a set of constraints matrices) of the learned constraint matrices with and without additional lifting functions is shown in Figure 11, and may give some intuition for why the higher-order terms help. We show the pattern aggregating all learned constraints of the problem without additional lifting functions (left), and with additional lifting functions (middle). More importantly, we show the pattern including only the constraints sufficient for tightness on the right. Comparing the sufficient pattern (right) with the insufficient pattern (left), we see that the elements corresponding to the

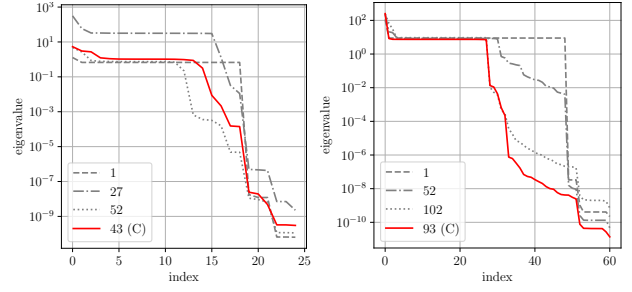


Fig. 9: Study of the singular value spectra of stereo localization problem in 2D (left) and 3D (right). Even after adding all found redundant constraints, a significant number of eigenvalues are nonzero. More higher-order Lasserre variables may be required to achieve rank-tightness. (See Figure 7 for a description of the labels.)

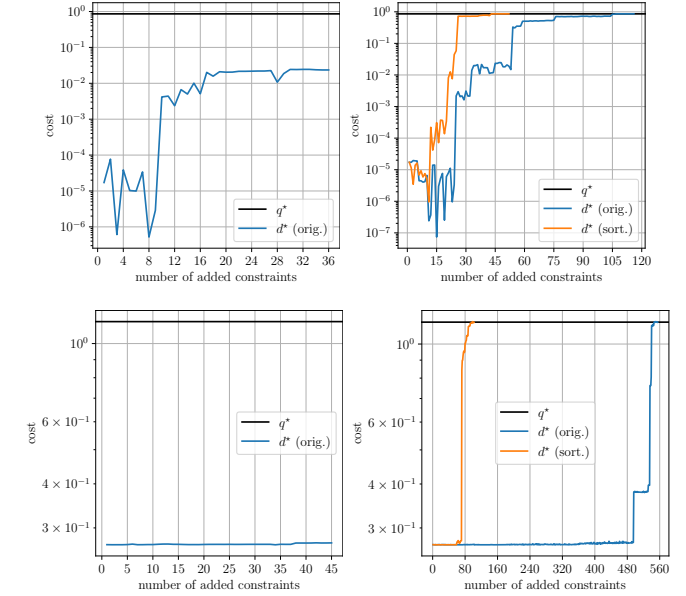


Fig. 10: Tightness study for stereo localization problem, using the original substitutions only (left) vs. the higher-order substitutions (right). The top and bottom row show the 2D and 3D case, respectively.

off-diagonal, nonzero elements of the cost matrix (circled in red) are populated when adding the lifting functions, which may help with meeting dual feasibility.

3) Generating Scalable Constraints (AUTOTEMPLATE):

The stereo localization problem presents two challenges for scalability of the learned constraints. First, there is the high dimensionality of the problem, in particular after adding the additional lifting functions required for tightness. Secondly, an investigation of the learned constraints, shown in Figure 12, suggests that many matrices actually depend on the (known) landmark coordinates and therefore do not generalize. We thus resort to AUTOTEMPLATE to scale to larger problem sizes. As explained in Section V-B, we use as parameters up to quadratic polynomials of each landmark's coordinates, and the considered variable groups are listed in Table II. At each level, we consider only the parameters touched by the considered variables. We achieve tightness after including all groups up to $\{l, \mathbf{z}_0, \mathbf{z}_1\}$ in both 2D and 3D. Figure 13 shows the output of the method (in compressed format), for the 2D example: a

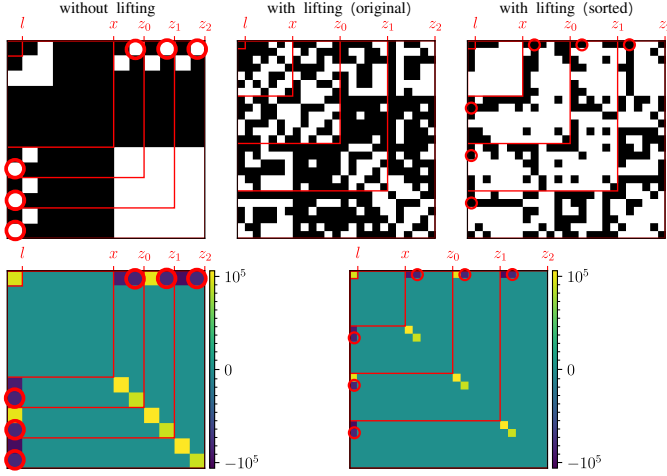


Fig. 11: Aggregate sparsity patterns (top row) and cost matrices (bottom row) of 2D stereo localization problem, using (from left to right) no higher-order lifting, higher-order lifting with original constraint matrix order, and higher-order lifting with order dictated by (25). Circled in red are off-diagonal elements that are not touched by any constraint matrices in the original form, but are touched in lifted form after sorting the matrices.

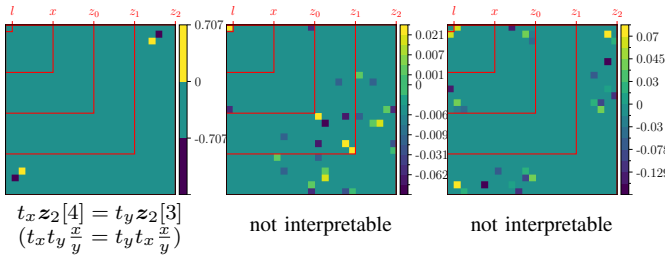


Fig. 12: Three learned constraint matrices for the 2D stereo localization problem. Many of the matrices are less sparse than in the range-only localization example and contain non-quantized numbers which suggests a dependency on landmark coordinates. Only few matrices, such as the one shown on the left, are interpretable (the identity is shown below the plot, where for simplicity, we call $\mathbf{t} = (t_x, t_y)^\top$, $\mathbf{T}\mathbf{m}_2 = (x, y, 1)^\top$, thus $\mathbf{u} = \frac{1}{y}(x, 1)^\top$ and $\mathbf{z}_2 = \frac{1}{y}(x, 1, t_x x, t_y x, t_x y, t_y y)^\top$).

set of templates over not only the original variables, but also their products with the parameters. The amount of constraints may seem unmanageable at first; but the templates can be significantly reduced by solving (V-D): only the highlighted constraints in Figure 13 are sufficient for tightness. Note also that thanks to factoring out the parameters, the matrix is now more quantized, with all nonzero elements in $\{\pm 1, \pm \frac{1}{\sqrt{2}}, \pm \frac{1}{2}\}$.

We successfully apply the patterns for up to 30 landmarks, as shown in Figure 14. For brevity, we discuss only the results of 3D localization. Again, we show how the times to create constraints and solve the SDP scale with N , and report the one-time cost of finding the sufficient set of templates in Table III. As for RO localization, the one-shot approach does not scale beyond $N = 10$ landmarks, while applying the reduced templates comes at a reasonable cost, comparable to the cost of solving the SDP itself. Compared to the much lower-dimensional RO localization problem, the performance here is not amenable to real-time applications yet. A more

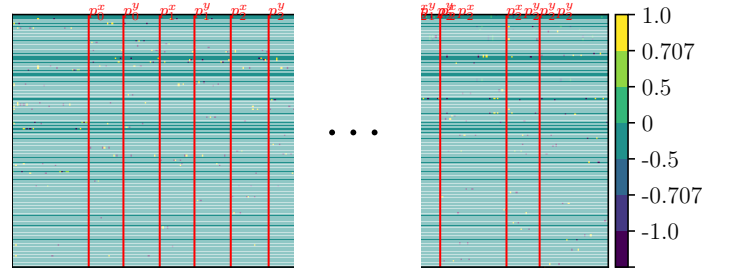


Fig. 13: Constraint templates learned for stereo-localization in 2D after factoring out parameters. The red bars delimit different parameter dependencies, with the left-most block corresponding to the original variables. Highlighted in dark are the 36 (out of 170) constraints sufficient for tightness.

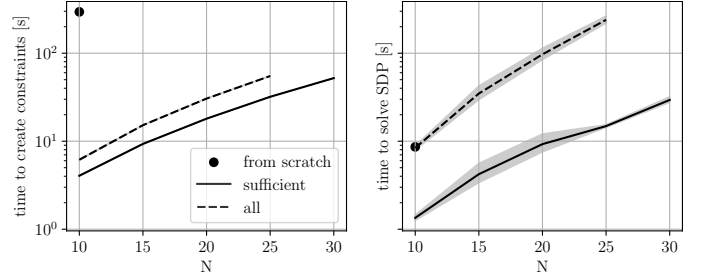


Fig. 14: Timing study of the stereo-localization problem in 3D as we increase the number of landmarks N . The labels are the same as in Figure 8. Learning constraints from scratch using AUTOTIGHT is prohibitively expensive even for $N = 10$. On the other hand, AUTOTEMPLATE scales reasonably up to $N = 30$.

efficient implementation of constraint creation than our un-optimized python code and advancements in speed of SDP solvers with redundant constraints would both be necessary for real-time performance on problems of reasonable size. However, the provided method is a step in the right direction: inputting the same problem formulation to the (sparse) Lasserre hierarchy tool provided by [7] leads to unmanageable numbers of variable and constraints, even for small problem sizes. For $d = 3$ and only $N = 3$ landmarks, a total of 27,692 trivially satisfied constraints are generated, which is far beyond what SDP solvers can currently handle in reasonable time. In contrast, we can go to as many as $N = 30$ landmarks, generating 18,320 or 4,733 linearly independent constraints when using all or only the sufficient templates, respectively.

D. Other Problems

We conclude by applying the proposed method to a number of problems from the literature whose semidefinite relaxations have been shown to be tight using certain redundant constraints. As a starting point, we consider two standard registration problems that have been treated by Briaies *et al.* [10], which are posed as standard least-squares problems over $SE(d)$: point-point registration (PPR) and point-line registration (PLR).

1) *PPR and PLR* [10]: In multimodal registration, the goal is to find an object's translation $\mathbf{t} \in \mathbb{R}^d$ and orientation $\mathbf{C} \in \mathbb{R}^d$ w.r.t. a world frame, given measurements of points lying on the object. The object is assumed to be represented by a

set of known geometric primitives of either points, lines, or planes. The problem is posed as the following minimization problem [10]:

$$\min_{C \in SO(d), t \in \mathbb{R}^d} \sum_{i=1}^N \|Cp_i + t - y_i\|_{W_i}^2, \quad (34)$$

with, respectively, $p_i \in \mathbb{R}^d$ and y_i the measured and an arbitrary point on the associated primitive P_i (note that data association is assumed known). The matrix $W_i \in \mathbb{R}^{d \times d}$ is chosen depending on the primitive P_i :

$$W_i = I_d \quad (\text{point}), \quad (35a)$$

$$W_i = I_d - v_i v_i^\top \quad (\text{line with unit direction } v_i), \quad (35b)$$

$$W_i = n_i n_i^\top \quad (\text{plane with normal } n_i). \quad (35c)$$

a) *Manual method [10]*: Problem (34) can be relaxed to a QCQP by dropping the determinant constraint from $SO(d)$ as explained in Section VI-C, and introducing $x^\top = [t^\top \text{vec}(C)^\top]$. The rank relaxation of this QCQP was shown to be always tight when using the following set of constraints [10]:

$$h^2 = 1 \quad (\text{prim., homogenization}), \quad (36a)$$

$$I_d = C^\top C \quad (\text{prim., orthonormal rows}), \quad (36b)$$

$$I_d = CC^\top \quad (\text{red., orthonormal columns}), \quad (36c)$$

$$c_{i|3} \times c_{i+1|3} = c_{i+2|3}, i \in [3] \quad (\text{red., handedness}), \quad (36d)$$

where ‘‘prim.’’ and ‘‘red.’’ are short for primary and redundant, $|$ is the modulo operator and c_i is the i -th column of C . This leads to a total of $1 + 2 \cdot 6 + 3 \cdot 3 = 22$ constraints in 3D, accounting for the symmetry of the optimization variable.

b) *Proposed method*: Our method finds the required redundant constraints outlined above, but without any manual steps. Figure 15 shows the discovered constraint matrices (in compressed form) by AUTOTIGHT. We find a total of 21 independent constraints, including the homogenization, suggesting that at least one of the 22 constraints presented by [10] are linearly dependent. Indeed, looking at the orthonormality constraints, we observe that out of the $3 + 3$ constraints that touch the diagonal in (36b) and (36c), respectively, only 5 are linearly independent. To see this, let us call $h_i(C) = 1$ the constraints touching the diagonal with $i \in \{1, 2, 3\}$ for (36b) and $i \in \{4, 5, 6\}$ for (36c). Then, it is easy to see that

$$\sum_{i=1}^3 h_i(C) = \sum_{i=4}^6 h_i(C), \quad (37)$$

so any of these six constraints can be written as a linear combination of the five others.

While these 21 constraints have been shown to be *sufficient* for tightness [10], they have not been shown to be *necessary*. In fact, we found that, for the considered noise level, none of the redundant constraints are required for PPR to be both cost- and rank-tight, as shown in Figure 16. For PLR, Figure 16 shows that the solution is in fact exactly rank two with only the seven primary constraints, but it becomes rank one after adding as few as two of the 12 available redundant constraints. Note that for this problem, we observed that the order of adding constraints did not make a difference.

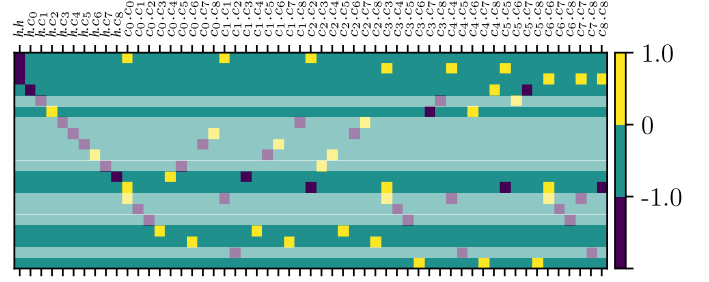


Fig. 15: Learned constraint templates for the multimodal registration problems [10]. The labels l and c_i correspond to the homogenization variable and the i -th element of $\text{vec}(C)$, respectively. We find that only 21 of the constraints suggested in [10] are actually linearly independent, see (37), and none of the redundant constraints are required for cost- and rank-tightness of point-point registration, while only a total of 10 (7 primary and 3 redundant) constraints, highlighted in dark, are required the point-line registration.

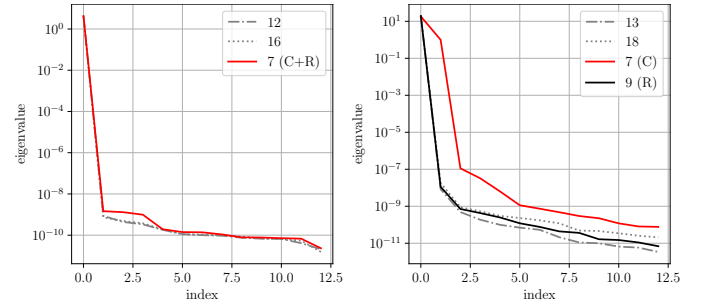


Fig. 16: Rank-tightness study for PPR (left) and PLR problems [10]. Both problems are cost-tight without redundant constraints, and for PLR, only 2 redundant constraints are required for tightness; a small subset of the 12 available redundant constraints [10].

2) *Robust estimation [7]*: Next, we consider two example problems treated by Yang *et al.* [7]: robust pointcloud registration and robust absolute-pose estimation. These two problems can in fact be seen as ‘robust’ variations of PPR and PLR, respectively, which is why we call them rPPR and rPLR, respectively.

Both rPPR and rPLR can be written in the form

$$\min_{\theta \in \mathcal{D}} \sum_{i=1}^N \rho(r(\theta, y_i)), \quad (38)$$

where \mathcal{D} is the domain of θ , ρ is a robust cost function and r the residual function. It is shown in [7] that for a vast selection of robust cost functions, residual functions, and domains, Problem (38) can be written as a QCQP. As an example, we focus on the truncated least-squares (TLS) cost function in what follows. The residual functions are given by

$$\text{rPPR: } r(\theta, y_i) = \|Cp_i + t - y_i\|^2, \quad (39)$$

$$\text{rPLR: } r(\theta, y_i) = \|Cp_i + t\|_{I_d - v_i v_i^\top}^2. \quad (40)$$

In rPPR, p_i and y_i are matched measurements of a pointcloud from different poses, while in $rPLR$, we assume p_i to be known landmark coordinates, and v_i unit vector measurements thereof, obtained for instance from a calibrated camera. The unknown state θ is again the pose $t \in \mathbb{R}^d, C \in SO(d)$. In order to satisfy the Archimedian condition, the authors further

restrict the domain \mathcal{D} to the domain with $\mathbf{t} \in \mathbb{R}^d$ contained in the ball of radius T .¹⁵ For the robust pose estimation problem, \mathbf{t} is also chosen so that the landmarks are in the field of view of the camera, characterized by aperture angle α . These two problems are thus examples with primary inequality constraints in (1).

a) *Manual method [7]*: For TLS cost, it has been shown that solving (38) is equivalent to solving [?]

$$\min_{\theta \in \mathcal{D}, \mathbf{w} \in \{\pm 1\}^N} \sum_{i=1}^N \frac{1 + w_i}{\beta_i^2} r^2(\theta, \mathbf{y}_i) + 1 - w_i, \quad (41)$$

where \mathbf{y}_i are measurements, \mathbf{w} is the vector of decision variables (for outliers, $w_i = -1$ and for inliers $w_i = 1$) and $\beta_i > 0$ are user-defined parameters determining the truncation threshold. Problem (41) can be written as a QCQP in the lifted vector

$$\mathbf{x}^\top = [h \quad \theta^\top \quad \mathbf{w}^\top \quad \mathbf{z}^\top], \quad (42)$$

with $\theta^\top = [\mathbf{t}^\top \text{vec}(\mathbf{C})^\top]$. The variable \mathbf{z} contains additional substitutions that are required to make Problem (41) quadratic in \mathbf{x} (the cost is cubic because the residual functions r are linear in θ). The authors propose to add the (sparse) Lasserre lifting function $\mathbf{z} = \theta \otimes \mathbf{w}$, which leads to a tight relaxation after adding a list of (trivially satisfied) constraints. The authors mention in passing that other lifting functions, such as $\mathbf{z} = \theta \otimes \theta$, which allow to write (41) as a QCQP, do not lead to a tight relaxation.

b) *Proposed method*: We study both lifting functions and come to the same conclusions as in [7]: both formulations allow for a large number of redundant constraints (which we found automatically), but only the second formulation becomes tight. Because of the large number of variables in the lifted state vector (using either of the two lifting functions), we resort directly to AUTOTEMPLATE. The variable ordering used (for both problems) can be found in Table II. When using the lifting function $\mathbf{z} := \theta \otimes \mathbf{w}$, the method terminates with cost-tightness after considering variables $\{l, \theta, \mathbf{z}_0, \mathbf{z}_1\}$. For $\mathbf{z} := \theta \otimes \theta$, the method returns that no tightness can be achieved.

The number of found and sufficient constraint templates can be found in Table III. We note that the number of required constraints is already very high when considering only $N = 4$ and $N = 6$ for rPPR and rPLR, respectively. Nevertheless, we can apply the templates to problems up to size $N = 15$, as shown in Figure 17. For both problems, learning constraints from scratch is prohibitively expensive. Thanks to the AUTOTEMPLATE method we can use the templates instead, and we obtain cost-tightness for all considered problems. Note that, just as in stereo localization, rank-tightness is not achieved and seems to not be computationally tractable since we already need many constraints for cost-tightness.

As a final observation, we compare the number of obtained constraints with the number of constraints found in [7] in Table IV. The results suggest that we find a significantly smaller subset of constraints, but without compromising tightness. We plan to further investigate this finding, taking a closer look at

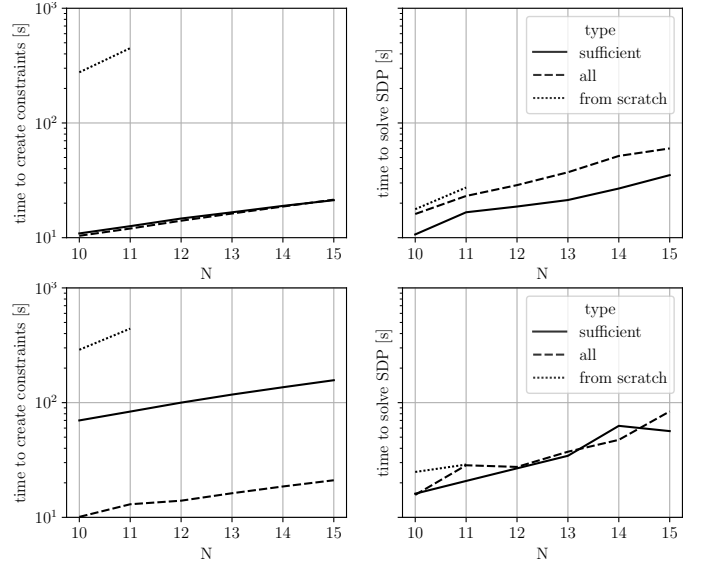


Fig. 17: Timing results of scaling to N landmarks for rPPR (top) and rPLR (bottom). Thanks to AUTOTEMPLATE we can automatically create the constraints of problems up to $N = 15$ landmarks.

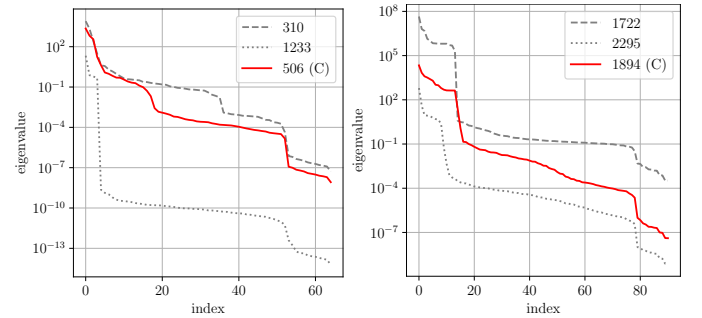


Fig. 18: Eigenvalue spectra for rPPR (left) and rPLR (right). We obtain cost-tightness, but not rank-tightness, for both problems.

the cost of solving the SDP using the different numbers of constraints, and investigating how rank-tightness is affected.

VII. CONCLUSION AND FUTURE WORK

We have presented new tools to find all possible redundant constraints for a given QCQP, which is paramount to tighten many semidefinite relaxations of problems encountered in robotics. The first tool, AUTOTIGHT, allows for the fast evaluation of given problem formulations, which we have used to evaluate different substitutions for range-only localization

TABLE IV: Comparison of the number of constraints found for rPPR and rPLR, respectively, using our method and the method proposed by [7], as a function of number of landmarks N .

N	rPPR		rPLR	
	our method	[7]	our method	[7]
10	4,508	6,257	5,330	7,379
11	5,293	7,398	6,279	8,724
12	6,139	8,633	7,304	10,180
13	7,046	9,962	8,405	11,747
14	8,014	11,385	9,582	13,425
15	9,043	12,902	10,835	15,214

¹⁵The Archimedean condition is a stronger form of compactness [41].

and stereo-based localization. After showing that we can find enough redundant constraints to achieve tightness for both problems, we have successfully used the second tool, AUTOTEMPLATE, to generalize the findings to new setups and larger problem sizes. To show their wide applicability, we have also showcased their performance on example problems from the literature [10, 7], showing that we find tight relaxations with even fewer redundant constraints than previously thought. As SDPs scale poorly with the number of constraints, this is a step in the right direction to make semidefinite relaxations scale to general problems encountered in robotics.

A number of follow-up questions deserve further attention. First, it was shown that both the measurement graph and the noise level can have an effect on tightness. In future work, we plan to investigate these characteristics using the given tool, and in particular understand to what level the additional redundant constraints may push the boundaries of tightness. Along the same lines, a given measurement graph may in fact help find the variable substitutions and parameters are most likely to succeed, a component of the proposed method that is currently defined by user input.

Finally, the full potential of the proposed method will be unlocked when faster SDP are developed for problems that require redundant constraints for tightness. First steps into this direction have shown promising results [6, 7, 12], but more work remains to be done. In parallel, there lies potential in further pushing the efficiency of optimality certificates of fast local solvers, for example using sampling-based approaches as in [18] or sparsity-exploiting approaches as in [33, 34].

REFERENCES

- [1] J. Rehder, J. Nikolic, T. Schneider, T. Hinzmann, and R. Siegwart, "Extending kalibr: Calibrating the extrinsics of multiple IMUs and of individual axes," in *IEEE International Conference on Robotics and Automation (ICRA)*. Stockholm, Sweden: IEEE, 2016, pp. 4304–4311.
- [2] T. D. Barfoot, *State Estimation for Robotics*. Cambridge University Press, 2017.
- [3] J. Nocedal and S. J. Wright, *Numerical Optimization*, 2nd ed., ser. Springer Series in Operations Research. Springer-Verlag, 2006.
- [4] A. Papalia, A. Fishberg, B. W. O'Neill, J. P. How, D. M. Rosen, and J. J. Leonard, "Certifiably Correct Range-Aided SLAM," *arXiv:2302.11614 [cs]*, 2023.
- [5] D. M. Rosen, L. Carlone, A. S. Bandeira, and J. J. Leonard, "SE-sync: A certifiably correct algorithm for synchronization over the special euclidean group," *International Journal of Robotics Research*, vol. 38, no. 2-3, pp. 95–125, 2019.
- [6] H. Yang, L. Liang, L. Carlone, and K.-C. Toh, "An Inexact Projected Gradient Method with Rounding and Lifting by Nonlinear Programming for Solving Rank-One Semidefinite Relaxation of Polynomial Optimization," *arXiv:2105.14033 [cs, math]*, no. arXiv:2105.14033, 2021.
- [7] H. Yang and L. Carlone, "Certifiably Optimal Outlier-Robust Geometric Perception: Semidefinite Relaxations and Scalable Global Optimization," *IEEE Transactions on Pattern Analysis and Machine Intelligence*, vol. 45, no. 3, pp. 2816–2834, 2023.
- [8] H. Yang, J. Shi, and L. Carlone, "TEASER : Fast and certifiable point cloud registration," *IEEE Transactions on Robotics*, vol. 32, no. 2, pp. 314–333, 2020.
- [9] A. Eriksson, C. Olsson, F. Kahl, and T.-J. Chin, "Rotation averaging and strong duality," in *IEEE/CVF Conference on Computer Vision and Pattern Recognition (CVPR)*, 2018, pp. 127–135.
- [10] J. Briales and J. Gonzalez-Jimenez, "Convex Global 3D Registration with Lagrangian Duality," in *IEEE Conference on Computer Vision and Pattern Recognition (CVPR)*. Honolulu, HI: IEEE, 2017, pp. 5612–5621.
- [11] S. Boyd and L. Vandenberghe, *Convex Optimization*. Cambridge University Press, 2004.
- [12] J. Wang and L. Hu, "Solving Low-Rank Semidefinite Programs via Manifold Optimization," *arXiv:2303.01722 [math]*, 2023.
- [13] J. B. Lasserre, "Global Optimization with Polynomials and the Problem of Moments," *SIAM Journal on Optimization*, vol. 11, no. 3, pp. 796–817, 2001.
- [14] J. P. Ruiz and I. E. Grossmann, "Using redundancy to strengthen the relaxation for the global optimization of MINLP problems," *Computers & Chemical Engineering*, vol. 35, no. 12, pp. 2729–2740, 2011.
- [15] A. Majumdar, R. Vasudevan, M. M. Tobenkin, and R. Tedrake, "Convex optimization of nonlinear feedback controllers via occupation measures," *International Journal of Robotics Research*, vol. 33, no. 9, pp. 1209–1230, 2014.
- [16] L. Sun and Z. Deng, "Certifiably Optimal and Robust Camera Pose Estimation From Points and Lines," *IEEE Access*, vol. 8, pp. 124 032–124 054, 2020.
- [17] J. Wang, V. Magron, and J.-B. Lasserre, "TSSOS: A Moment-SOS Hierarchy That Exploits Term Sparsity," *SIAM Journal on Optimization*, vol. 31, no. 1, pp. 30–58, 2021.
- [18] D. Cifuentes and P. A. Parrilo, "Sampling algebraic varieties for sum of squares programs," *SIAM Journal on Optimization*, vol. 27, no. 4, pp. 2381–2404, 2017.
- [19] C. Olsson, F. Kahl, and M. Oskarsson, "Branch-and-Bound Methods for Euclidean Registration Problems," *IEEE Transactions on Pattern Analysis and Machine Intelligence*, vol. 31, no. 5, pp. 783–794, 2009.
- [20] R. Hartley, J. Trumpf, and D. H. Li, "Rotation averaging," *International Journal of Computer Vision*, vol. 103, no. 3, pp. 267–305, 2013.
- [21] L. Brynte, V. Larsson, J. P. Iglesias, C. Olsson, and F. Kahl, "On the Tightness of Semidefinite Relaxations for Rotation Estimation," *Journal of Mathematical Imaging and Vision*, vol. 64, no. 1, pp. 57–67, 2022.
- [22] J. Briales, L. Kneip, and J. Gonzalez-Jimenez, "A Certifiably Globally Optimal Solution to the Non-minimal Relative Pose Problem," in *IEEE/CVF Conference on Computer Vision and Pattern Recognition (CVPR)*. Salt Lake City, UT: IEEE, 2018, pp. 145–154.
- [23] D. Cifuentes, "A Convex Relaxation to Compute the Nearest Structured Rank Deficient Matrix," *SIAM Journal on Matrix Analysis and Applications*, vol. 42, no. 2, pp. 708–729, 2021.
- [24] K. Anstreicher and H. Wolkowicz, "On Lagrangian Relaxation of Quadratic Matrix Constraints," *SIAM Journal on Matrix Analysis and Applications*, vol. 22, no. 1, pp. 41–55, 2000.
- [25] E. Wise, M. Giamou, S. Khoubyarian, A. Grover, and J. Kelly, "Certifiably Optimal Monocular Hand-Eye Calibration," in *IEEE International Conference on Multisensor Fusion and Integration for Intelligent Systems (MFI)*, 2020, pp. 271–278.
- [26] J. Zhao, W. Xu, and L. Kneip, "A Certifiably Globally Optimal Solution to Generalized Essential Matrix Estimation," in *IEEE/CVF Conference on Computer Vision and Pattern Recognition (CVPR)*, 2020, pp. 12 034–12 043.
- [27] T. Marucci, J. Umenberger, P. A. Parrilo, and R. Tedrake, "Shortest Paths in Graphs of Convex Sets," *arXiv:2101.11565 [cs, math]*, 2022.
- [28] T. Marucci, M. Petersen, D. von Wrangel, and R. Tedrake, "Motion Planning around Obstacles with Convex Optimization," *arXiv:2205.04422 [cs]*, 2022.
- [29] S. Burer and R. D. Monteiro, "Local Minima and Convergence in Low-Rank Semidefinite Programming," *Mathematical Programming*, vol. 103, no. 3, pp. 427–444, 2005.
- [30] N. Boumal, "A Riemannian low-rank method for optimization over semidefinite matrices with block-diagonal constraints," *arXiv:1506.00575 [cs, math, stat]*, 2016.
- [31] K. J. Doherty, D. M. Rosen, and J. J. Leonard, "Performance Guarantees for Spectral Initialization in Rotation Averaging and Pose-Graph SLAM," *arXiv:2201.03773 [cs]*, 2022.
- [32] F. Dellaert, D. M. Rosen, J. Wu, R. Mahony, and L. Carlone, "Shonan rotation averaging: Global optimality by surfing $\{\text{SSO}(p)\}$," in *European Conference on Computer Vision*, 2020, pp. 292–308.
- [33] C. Holmes and T. D. Barfoot, "An Efficient Global Optimality Certificate for Landmark-Based SLAM," *IEEE Robotics and Automation Letters*, vol. 8, no. 3, pp. 1539–1546, 2023.
- [34] F. Dümbgen, C. Holmes, and T. D. Barfoot, "Safe and Smooth: Certified Continuous-Time Range-Only Localization," *IEEE Robotics and Automation Letters*, vol. 8, no. 2, pp. 1117–1124, 2023.
- [35] Á. Parra, S.-F. Chng, T.-J. Chin, A. Eriksson, and I. Reid, "Rotation Coordinate Descent for Fast Globally Optimal Rotation Averaging," in *IEEE/CVF Conference on Computer Vision and Pattern Recognition (CVPR)*, 2021, pp. 4296–4305.
- [36] B. Buchberger, "An algorithm for finding the basis elements of the residue class ring of a zero dimensional polynomial ideal," Ph.D. dissertation, Johannes Kepler University of Linz, 1965.

- [37] S. Shen and R. Tedrake, “Sampling Quotient-Ring Sum-of-Squares Programs for Scalable Verification of Nonlinear Systems,” in *IEEE Conference on Decision and Control (CDC)*, 2020, pp. 2535–2542.
- [38] MOSEK. ApS, *The MOSEK Optimization Toolbox for MATLAB Manual. Version 10.0.*, 2022.
- [39] D. Cifuentes, S. Agarwal, P. A. Parrilo, and R. R. Thomas, “On the local stability of semidefinite relaxations,” *Mathematical Programming*, no. 193, pp. 629–663, 2022.
- [40] A. Beck, P. Stoica, and J. Li, “Exact and Approximate Solutions of Source Localization Problems,” *IEEE Transactions on Signal Processing*, vol. 56, no. 5, pp. 1770–1778, 2008.
- [41] G. Blekherman, P. A. Parrilo, and R. Thomas, *Semidefinite Optimization and Convex Algebraic Geometry*. MOS-SIAM Series on Optimization, 2012, vol. 13.
- [42] T. F. Coleman and A. Pothén, “The Null Space Problem I. Complexity,” *SIAM Journal on Algebraic Discrete Methods*, vol. 7, no. 4, pp. 527–537, 1986.
- [43] G. H. Golub and C. F. Van Loan, *Matrix Computations*, 4th ed. The John Hopkins University Press, 2003.
- [44] M. W. Mueller, M. Hamer, and R. D’Andrea, “Fusing ultra-wideband range measurements with accelerometers and rate gyroscopes for quadcopter state estimation,” in *IEEE International Conference on Robotics and Automation (ICRA)*, 2015, pp. 1730–1736.
- [45] A. Goudar, W. Zhao, T. D. Barfoot, and A. P. Schoellig, “Gaussian Variational Inference with Covariance Constraints Applied to Range-only Localization,” in *IEEE/RSJ International Conference on Intelligent Robots and Systems (IROS)*, 2022, pp. 2872–2879.
- [46] F. Zafari, A. Gkelias, and K. K. Leung, “A Survey of Indoor Localization Systems and Technologies,” *IEEE Communications Surveys & Tutorials*, vol. 21, no. 3, pp. 2568–2599, 2019.
- [47] L. Matthies and S. Shafer, “Error modeling in stereo navigation,” *IEEE Journal on Robotics and Automation*, vol. 3, no. 3, pp. 239–248, 1987.
- [48] G. Terzakis and M. Lourakis, “A Consistently Fast and Globally Optimal Solution to the Perspective-n-Point Problem,” in *European Conference on Computer Vision*, A. Vedaldi, H. Bischof, T. Brox, and J.-M. Frahm, Eds., 2020, pp. 478–494.
- [49] S. Diamond and S. Boyd, “CVXPY: A Python-Embedded Modeling Language for Convex Optimization,” *Journal of Machine Learning Research*, vol. 17, pp. 1–5, 2016.
- [50] A. Agrawal, R. Verschueren, S. Diamond, and S. Boyd, “A rewriting system for convex optimization problems,” *Journal of Control and Decision*, vol. 5, no. 1, pp. 42–60, 2018.
- [51] J. Townsend, N. Koep, and S. Weichwald, “Pymanopt: A Python Toolbox for Optimization on Manifolds using Automatic Differentiation,” *Journal of Machine Learning Research*, vol. 17, no. 137, pp. 1–5, 2016.
- [52] C. Liu and N. Boumal, “Simple algorithms for optimization on Riemannian manifolds with constraints,” *arXiv:1901.10000 [math]*, 2019.